RPP-RPT-60893
Revision 0

LAW Glass Testing by Long-Term PCT to Support Disposal at IDF

Prepared by

Authors
Elvie Brown
Washington River Protection Solutions, LLC

Isabelle S. Muller and Ian L. Pegg
Vitreous State Laboratory, The Catholic University of America, Washington, DC

Date Published
09/28/2017

Prepared for the U.S. Department of Energy
Office of River Protection

Contract No. DE-AC27-08RV14800

VSL-17R4320-1

Final Report

LAW Glass Testing by Long-Term PCT to Support Disposal at IDF

prepared by

Isabelle S. Muller and Ian L. Pegg

Vitreous State Laboratory
The Catholic University of America
Washington, DC 20064

for

Atkins Energy Federal EPC, Inc.
Calverton, MD 20705

and

Washington River Protection *Solutions*, LLC
Richland, WA

July 17, 2017

Rev. 0, 09/28/17

Completeness of Testing:

This report describes the results of work and testing specified by WRPS. The work and any associated testing followed established quality assurance requirements. The descriptions provided in this test report are an accurate account of both the conduct of the work and the data collected. Results required by the test program are reported. Also reported are any unusual or anomalous occurrences that are different from the starting hypotheses. The test results and this report have been reviewed and verified.

I. L. Pegg: I. Pegg **Date:** 9/28/17
VSL Program Director/Principal Investigator

I. Joseph: Innocent Joseph **Date:** 9/28/17
Atkins Sub-Contract Manager

TABLE OF CONTENTS

List of Tables

List of Figures

List of Abbreviations

ANL-LRM	Argonne National Laboratory – Low-Activity Waste Reference Material
ASME	American Society of Mechanical Engineers
ASTM	American Society for Testing and Materials
CCC	Canister Centerline Cooling
CERCLA	Comprehensive Environmental Response, Compensation, and Liability Act
CUA	The Catholic University of America
DCP-AES	Direct Current Plasma Atomic Emission Spectroscopy
DOE	Department of Energy
EDS	Energy Dispersive X-Ray Spectroscopy
HLW	High Level Waste
ICDD	International Centre for Diffraction Data
IDF	Integrated Disposal Facility
ILAW	Immobilized Low Activity Waste
IHLW	Immobilized High Level Waste
LAW	Low Activity Waste
LFRG	Low Level Waste Disposal Facility Federal Review Group
ORP	Office of River Protection
PCT	Product Consistency Test
PA	Performance Assessment
PNNL	Pacific Northwest National Laboratory
PUF	Pressurized Unsaturated Flow Test
NQA	Nuclear Quality Assurance
QARD	Quality Assurance Requirements and Description
RCRA	Resource Conservation and Recovery Act
ROD	Record of Decision
S/V	Surface to Volume Ratio
SEM	Scanning Electron Microscopy
SPFT	Single-Pass Flow-Through (Test)
TC&WM EIS	Tank Closure & Waste Management Environmental Impact Statement
TST	Transition State Theory
VHT	Vapor Hydration Test
VSL	Vitreous State Laboratory
WRPS	Washington River Protection *Solutions*, LLC
WTP	Hanford Tank Waste Treatment and Immobilization Plant
XRD	X-Ray Diffraction
XRF	X-Ray Fluorescence Spectroscopy

SECTION 1.0
INTRODUCTION

1.1 Background

About 50 million gallons of high-level mixed waste is currently stored in underground tanks at The United States Department of Energy's (DOE's) Hanford site in the State of Washington. The Hanford Tank Waste Treatment and Immobilization Plant (WTP) will provide DOE's Office of River Protection (ORP) with a means of treating this waste by vitrification for subsequent disposal. The tank waste will be separated into low- and high-activity waste fractions, which will then be vitrified respectively into Immobilized Low Activity Waste (ILAW) and Immobilized High Level Waste (IHLW) products. The ILAW product will be disposed in an engineered facility – the Integrated Disposal Facility (IDF) – on the Hanford site, while the IHLW product is designed for a national deep geological disposal facility for high-level nuclear waste. The ILAW and IHLW products must meet a variety of requirements with respect to protection of the environment before they can be accepted for disposal.

The Record of Decision (ROD) from the Tank Closure & Waste Management Environmental Impact Statement (TC&WM EIS) establishes the current waste streams to be disposed of at the IDF to be located in the 200 East Area which include ILAW, secondary waste associated with ILAW production, and other on-site Hanford non- Comprehensive Environmental Response, Compensation, and Liability Act (CERCLA) waste. In accordance with the DOE order on radioactive waste management (DOE Order 435.1), the IDF performance assessment (PA) is intended to analyze the long-term impacts on human health and the environment of the disposition of waste placed into the facility. Evaluation of the impact of disposed waste requires the ability to predict the long-term release of key radionuclides from the engineered system. In the case of IDF, the engineered system includes a number of components including the proposed Resource Conservation and Recovery Act (RCRA) cap, back fill material, ILAW glass, leachate collection system, etc.

Since 1998, the IDF PA (formerly the ILAW PA) has been supported by a PA maintenance plan focused on collecting the critical data needed to predict long-term performance: site geology, recharge, hydrology, geochemistry (measurement of site specific K_d values for key contaminants of concern), and waste form release. The purpose of the PA maintenance plan is to allow PA revisions to reflect new scientific information that reduces the technical uncertainty associated with critical aspects of the PA. Although many of the components contained in the engineered system and addressed in previous IDF PAs are important in minimizing radionuclide release, arguably the most important, protective, and uncertain aspect of the engineered system is the long-term performance of the ILAW glass. The ILAW glass serves as a primary barrier that controls radionuclide release. Therefore, developing robust, scientifically defensible predictions of long-term glass performance for the IDF PA is

critical. The technical approach that is currently used to predict long-term release from ILAW glass for the IDF PA has gained acceptance from the Low-Level Waste Disposal Facility Federal Review Group (LFRG) and the international community evaluating the long-term corrosion of waste glass [1-3]. It has also been peer reviewed and approved by a panel of independent experts during development of the 1998 IDF PA.

In the early IDF PAs, three prototypic glasses that spanned the range of glass compositions expected to be produced by the WTP were selected based upon specific processing constraints and composition projections that were current at the time. However, subsequent work has expanded the range of glass compositions that may be produced at the WTP and this type of composition range expansion is likely to continue through the life of the project. Thus, while the basic technical approach is well developed, there was a need to expand the range of glasses tested in order to span the composition range expected to be disposed in the IDF, and to develop an understanding of the dependence of the underlying model parameters and reaction network on the ILAW glass composition. Washington River Protection *Solutions*, LLC (WRPS) is leading the work to address this need and contracted with Atkins and the Vitreous State Laboratory (VSL) of The Catholic University of America (CUA) to provide scientific and technical support. The work was initiated in FY 2015 in response to the corresponding WRPS scope of work [4]. The present document provides results from the sampling and analysis of leachates from leach tests that are on-going and for which yet longer-term data will be obtained. For convenience, much of the background information provided in previous reports is repeated here.

1.2 ILAW Release Approach for the IDF PA

The technical approach that is currently used to predict long-term release from ILAW glass for the IDF PA has been developed, refined, and updated over the past decade or so. The approach and the supporting test data for ILAW glasses have been extensively documented [3, 5 - 14]. A brief summary is presented in this section.

The underlying premise of the IDF PA is that the source term for radionuclide release is controlled by the long-term weathering of the glass matrix. This engineering-based approach has been used in previous PAs to provide the defense-in-depth required to defend the above premise and demonstrate through computer simulations that the proposed glass waste form will meet the regulatory requirements put forth by the LFRG. The focus of this engineering-based approach is estimating the model parameters and chemical reaction network needed to provide a robust simulation of glass weathering and the corresponding release of radionuclides over the period of performance (~10,000 years). The model parameters, $\vec{k}_o, \eta, E_a, K_g,$ and r_{IEX}, are used to populate a chemical affinity-based kinetic rate law that is based upon Transition State Theory (TST) [5, 15]:

$$r = \vec{k}_o 10^{\eta pH} \exp\left(\frac{-E_a}{RT}\right)\left[1-\left(\frac{Q}{K_g}\right)\right]^{\sigma} + r_{IEX}\,(\qquad (1)$$

where r is the dissolution rate [g/(m^2 d)], $\bar{k}_o$ is the forward rate constant [g /(m^2 d)], pH is equal to negative $\log_{10}$ of the hydrogen ion activity, η is the power law coefficient, E_a is the apparent activation energy (kJ/mol), R is the gas constant [kJ/(mo1 K)], T is the temperature (K), Q is the ion activity product (unitless), K_g is the pseudo-equilibrium constant for the rate controlling phase or phases (unitless), and σ is the Temkin coefficient, which has been theoretically shown to equal one. Equation (1) relates the effect of: (1) pH, (2) temperature, (3) saturation state of the system, and (4) the activities of species that affect the rate of glass dissolution via Q. Equation (1) is based on the kinetic rate equation developed by Åagaard and Helgeson [16], as applied to glass by Grambow [17] wherein orthosilicic acid is the only rate controlling species in Q. In addition to the TST rate equation, an additional term has been added to the IDF PA calculations to predict the ion-exchange rate (r_{IEX}) as the glass-water reaction proceeds. The r_{IEX} is a function of temperature, glass composition, and reaction progress (stage of the glass-water reaction). The potential importance of the contribution from ion exchange had been emphasized previously [6, 18-20].

The use of Equation (1) with suitably estimated parameters allows for the source-term to be estimated within a reactive chemical transport modeling framework that takes into account the coupled effects of fluid flow and glass-water reactions on the chemistry of fluids percolating through the disposal facility. Coupling the fluid chemistry with a kinetic rate equation allows the simulations to describe the response of the glass corrosion rate to changes in fluid composition as a function of time and space.

In previous work, the model parameters for Equation (1) have been obtained from the analysis of data produced using a variety of experimental techniques, including the single-pass flow through test (SPFT), long-term high surface to volume ratio (S/V) product consistency test (PCT-B), vapor hydration test (VHT), and pressurized unsaturated flow test (PUF). This suite of tests evaluates different aspects of the glass-water reaction over the course of the various regimes of glass weathering: the initial forward rate regime; the decreasing rate regime; the residual rate regime; and the alteration rate renewal regime. These regimes are described below.

The initial forward rate consists of both ion-exchange and hydrolysis reactions. In dilute to near-saturated solutions, the TST-based model (without the ion-exchange term) successfully accounts for silicate dissolution in terms of temperature, pH, and reactive surface area when hydrolysis is the controlling reaction. However, as the glass-water reaction proceeds and the concentration of glass components (particularly the dissolved silicic acid concentration) increases in solution, the rate of dissolution decreases. For ILAW glasses tested under alkaline conditions, it has been observed that ion exchange becomes the dominant process controlling glass weathering under these near-saturated conditions, as was pointed out earlier for high-level waste (HLW) glasses [20]. The data collected from SPFT experiments conducted as a function of pH, temperature, and silicic acid concentration are used to study these processes and to obtain the model parameters $\bar{k}_o$, η, E_a, and K_g.

As the glass continues to dissolve, the aqueous concentration of dissolved components approaches saturation with respect to the formation of a hydrated surface layer. The combined H^+/Na^+ inter-diffusion and hydrolysis of the silicate network lead to the formation of a multi-layered reaction zone including a hydrated layer, a porous gel layer, and crystalline phases that precipitate on the surface. Increasing the S/V (e.g., in PCT-B) is one method to explore higher reaction progresses and identify the secondary phases that are associated with resumption.

The hydrated surface layer forms either as a reorganization of the hydrated layer (phylosilicates) or when relatively insoluble glass components (e.g., Al, Fe, and Si) accumulate in the bulk solution and precipitate at the glass-water interface (tectosilicate) [21, 22]. The water-glass interface is a multi-layer system that includes phases in which the less soluble components left behind are organized into a hydrated layer of phyllosilicates and tectosilicates from the precipitation of components in solution that exceed the solubility limit [21]. The rate of dissolution then continues at a relatively constant residual rate that has been shown in some cases to be consistent with a process controlled by diffusion through the hydrated surface layer. The key alteration phase is often a clay mineral, such as a smectite or chlorite. The precipitation kinetics associated with these phases can be complex, but in general, the rate of secondary phase growth increases in response to an increase in the magnitude of supersaturation [23, 24]. The data collected from SPFT experiments conducted as a function of temperature and silicic acid concentration can be used to evaluate the residual rate and obtain the model parameter r_{IEX}.

Finally, depending on the type of alteration phases that form, the glass-water reaction can increase from the residual rate and return to an elevated rate, which is termed resumption. This type of behavior has been observed in accelerated testing of various glasses including US HLW glasses [25-29], other HLW glasses [30-40], as well as Hanford low-activity waste (LAW) glasses [14, 28, 41, 42].

The data collected from VHT, PCT-B, and PUF experiments along with geochemical modeling and solid-phase characterization are used to identify the key alteration phases formed as the glass weathers. The results from these tests provide the additional confirmatory information needed to identify and constrain the appropriate chemical reaction network required for model simulations.

1.3 Previous Testing at VSL

A large data set of results from long-term PCT-B (American Society for Testing and Materials (ASTM) C1285) testing performed at VSL on WTP LAW glasses was compiled and reported previously [14]. The data set includes glass compositions, leachate compositions and pH at each sampling interval, sampling time, test condition (leachant, temperature, S/V, test protocol, etc.), and associated secondary phase information. Data for a total of 253 LAW glass compositions are included in the data set, which extends up to 3982 days of PCT-B leaching.

These glass formulations were developed at VSL in support of the WTP and provided the basis for the present WTP baseline formulations. These glasses span a composition range that is much more extensive than those used in previous performance assessment glass testing work [10]. Selected tests were sampled and analyzed to characterize the secondary phases, which included zeolites such as analcime and phillipsite and phyllosilicates of the smectite group, stevensite and swinefordite [14]. Glasses in the later stages of the reaction progress were included in this analysis.

In addition to the development of the baseline operating envelope for the WTP, since 2003, VSL has been developing a wide range of LAW formulations that achieve considerably higher waste loadings than the WTP baseline formulations [43-45]. As a result, the range of glass compositions that may be produced at the WTP is expanding toward higher sodium and sulfate contents and new glass components such as V_2O_5 (for improved sulfate solubility), SnO_2 (for leach resistance at high alkali concentrations), and Cr_2O_3 (for resistance to K-3 refractory corrosion) that are added as glass former additives, and this type of composition range expansion is likely to continue through the life of the project. In an initial effort to begin to encompass the composition range expected to be disposed at the IDF, a total of 10, referred to as IDF Phase 1 glasses, were selected as bounding glasses for this composition expansion [14]. The compositions of these glasses are presented in Table 2.1 and discussed in Section 2. The selection was based on an analysis of the compositions and properties of the large number of LAW glasses that have been developed for the WTP at VSL. Multiple batches of these ten selected glasses were prepared for testing at VSL. Samples of three of these glasses were also shipped to Pacific Northwest National Laboratory (PNNL) to support complementary PUF testing (IDF1-B2, IDF2-G9, and IDF3-F7). All ten of these glasses were subjected to PCT-B at VSL at three temperatures (40°C, 90°C and 120°C) and two S/V values (2,000 m^{-1} and 20,000 m^{-1}). The results showed that although the LAW glasses selected for this evaluation are compositions that have higher waste loadings than those developed for the WTP baseline, they follow generally similar leaching behavior. It is also evident that an increase in total alkali content alone is not necessarily detrimental to long-term PCT leaching. Furthermore, glass IDF1-B2, which has the highest alkali content of all ten glasses, and which fails the WTP VHT requirement by a significant margin, was actually one of the better performing glasses over the range of PCT-B conditions investigated. Glass IDF1-B2 showed robustness with respect to rate resumption despite increases in test temperature and S/V, both of which promote more interactive leaching conditions that drive the system towards secondary phase formation. This glass was deliberately included in the study to provide such a bounding case, together with the other IDF Phase 1 glasses described above; the rationale for the selection of these glasses has been described previously [14].

Four of the ten selected glasses were also subjected to SPFT testing (ASTM C1662) at VSL; the results were reported earlier [14, 46]. Full-suites of SPFT experiments as a function of pH, temperature, and silicic acid concentration (48 tests) were performed on the selected bounding glass, IDF1-B2 and on glass IDF7-E12. More limited SPFT tests as a function of silicic acid concentration and temperature were performed on two other glasses, IDF2-G9 and

IDF3-F7. Subsequently a full suite of SPFT tests was conducted on glass IDF2-G9 at PNNL [47]. The selected bounding glass IDF1-B2 has a high Na_2O concentration (25 wt%) that significantly exceeds that of the WTP baseline glasses; it also has properties that challenge but are within the WTP limits except for its VHT response. The results of the SPFT tests were analyzed to determine the parameters in the ILAW glass dissolution model [14]. The rate law parameters were generally similar to those for the previously tested WTP baseline glasses but a number of deviations from that model were identified and discussed [14, 46]. For example, the results suggest that the kinetic rate law model previously used for the ILAW PA exhibits variable degrees of success depending on the specific experimental conditions. The model worked well for IDF1-B2 tests performed far from saturation but under near saturation conditions, there was a correlation between experimentally obtained and calculated dissolution rates for glass IDF1-B2 only at low temperatures. The results also suggest that there may be important limitations on the use of boron release rate as a reliable indicator of the overall glass reaction rate [14, 46].

The rate law parameters determined from the SPFT tests on these four high waste loading glasses are in good agreement with those determined for other LAW glasses, such as LAWA44, LAWB45, and LAWC22, which are baseline WTP formulations that have generally lower waste loadings and, therefore, lower alkali contents (based on the values reported in [48] which corrected the errors in the previously reported values [10]). The fact that the rate law parameters determined for the bounding glass are close to those for the more typical WTP glasses is of practical significance since it suggests that higher waste loading glasses such as IDF1-B2 will likely still meet the requirements of the IDF PA. Establishing the viability of such high waste loading glasses in this regard is important in realizing their potential benefits in terms of reductions in life cycle costs and mission duration.

The results from long-term PCT-Bs collected at VSL over the previous five years for the ten Phase 1 glasses and an update of sampling and analyses for the period of December 2015 to August 2016 were reported earlier [49, 50]. The data were collected at an S/V of 20,000 m^{-1} (90°C) over 272 days, as well as at the nominal PCT S/V of 2000 m^{-1} at temperatures of 90°C and 40°C over 1800 days (tests were also performed at 120°C but all data were reported in 2011 [14] and the tests were terminated). At the lower temperature of 40°C, the greatest extent of reaction based on boron normalized leaching was for glass IDF8-A125CCC, which reached 10 to 11% reacted glass at 900 days; that glass has stabilized at this level with little further alteration over the past 3 years. At 90°C, IDF9-A187CCC and IDF6-D6CCC were the first to reach resumption (after one year at S/V of 2000 m^{-1} and after 2 months at S/V of 20,000 m^{-1}). IDF7-E12CCC shows similar resumption at around 1200 days at S/V of 2000 m^{-1} and 120 days at S/V of 20,000 m^{-1}. Glass IDF4-A15CCC at 90°C and S/V of 2000 m^{-1} shows similar resumption starting at about 1200 days although a slower rise was evident as early as 272 days at 90°C and S/V of 20,000 m^{-1}. Glass IDF8-A125CCC shows resumption beginning at about 570 days but the rate of rise is somewhat lower than for the other glasses (90°C, S/V 2,000 m^{-1}).

Selected PCTs were sampled and analyzed to characterize the secondary phases, which included zeolites such as analcime and gobbinsite, and phyllosilicates of the smectite group,

saponite, lizardite, tobermorite and kaolinite. Glasses that have reached the later stages of reaction progress show the most abundant secondary phases, which facilitate their identification. High alumina and low ZrO_2 are compositional characteristics of these glasses. Glasses IDF4-A15CCC, and IDF5-A20CCC are among those with relatively high total alkali content. Of these, IDF4-A15CCC has reached resumption and shows the phase phillipsite in the alteration products. Conversely, IDF5-A20CCC has not yet reached resumption and shows only gehlenite in the alteration products. IDF3-F7CCC has similar total alkali content to IDF7-E12CCC. While IDF7-E12CCC has reached resumption, IDF3-F7CCC has showed no resumption or any detectable alteration phases after 5 years (90°C and S/V 2000 m^{-1}). In addition to glass IDF3-F7CCC, glasses IDF2-G9CCC and IDF10-Zr6CCC have also shown no resumption to date in any of the tests. These glasses have the highest Li, the highest K, and the highest Zr contents, respectively.

Results on PCT-B for the ten Phase 2 glasses subjected to long-term PCT-B at 90ºC and S/V of 20,000 m^{-1} were also previously reported for up to 365 days of sampling [49, 50]. The compositions of these glasses are presented in Table 2.2. Four of these glasses had reached resumption within a year of leaching at the following respective times: IDF18-A161CCC (180 days), IDF19-C100CCC (273 days), IDF14-A59CCC (272 days), and IDF15-A57CCC (365 days). One notable compositional characteristic of these glasses is that they have lower ZrO_2 contents among the Phase 2 glasses.

Overall the PCT-B results collected so far show that although the LAW glasses selected for this evaluation have higher waste loadings than those developed for the WTP baseline, they follow generally similar leaching behavior and the increase in total alkali content alone is not necessarily detrimental to long-term PCT leaching. After five-year leach testing, glass IDF1-B2CCC, which has the highest alkali content on a molar basis of all 20 glasses and which fails the WTP VHT requirement by a significant margin, is still one of the better performing glasses over the range of PCT-B conditions investigated. This glass was deliberately included in the present study to provide such a bounding case. Based on the results available at present, the most detrimental compositional features in terms of early resumption appear to be high alumina and lower zirconia and silica.

Many of the long-term PCT-Bs initiated in Phase 1 and all of the long-term PCT-Bs initiated on the ten Phase 2 glasses are still ongoing. The present report provides a discussion of results relating to sampling and analyses of these long-term PCTs as well as collection and analysis of representative samples of the reacted Phase 2 glasses and associated secondary phases.

SECTION 2.0
DESCRIPTION OF IDF GLASSES

The target compositions of the selected Phase 1 and Phase 2 LAW glasses are given in Tables 2.1 and 2.2, respectively. They were selected from ORP-LAW glasses with higher waste loadings and the majority of them have been tested for processability in a DM10 or DM100 melter, as shown in Figure 2.1 (marked as ORP Melter Tests). A few glasses that have been tested only at crucible scale were included to better cover the compositional space for LAW glass compositions. XRF measured SO_3 values from the crucible glass melts prepared for IDF tests [49] are used to define the SO_3 content of these glasses. Their compositions in elemental percentage along with a summary of their properties are given in Table 2.3. Short descriptions of these glasses are given below.

- IDF1-B2, based on ORPLB2 (25.0 wt% Na_2O, 0.1 wt% K_2O, 0.5 wt% SO_3) has the highest mol% alkali oxide content among the selected glasses. This glass shows K-3 refractory corrosion neck loss close to the limit of 0.04 inches and VHT alteration rate slightly more than double the WTP limit (Figure 2.2). Among the glasses evaluated for selection at the highest Na_2O content, three shown in Figure 2.2 (ORPLA5, ORPLA6 and ORPLA7) have viscosity values outside of the acceptable WTP upper limit of 150 poise at 1100°C. Another glass (LAWA195) shows about 3 vol% crystals after heat treatment for 20 hours at 950°C. Of the glasses containing 25 wt% Na_2O, ORPLB2 is one for which properties relevant to processing are close to but within the WTP limits, PCT releases within the WTP limits, and only VHT is above the WTP limit; it was therefore selected as the bounding glass composition for the full suite of SPFT testing and PCT-B.
- IDF2-G9, based on ORPLG9 (21.0 wt% Na_2O, 5.8 wt% K_2O) was selected from the high alkali-high potassium glasses (see Figure 2.3). This glass shows K-3 corrosion neck loss and VHT alteration rate close to, but within WTP limits. This glass was selected for partial SPFT testing and PCT-B. The sample had not reached resumption based on PCT-B results at up to seven years at 90°C and S/V of 2,000 m^{-1}.
- IDF3-F7, based on ORPLF7 has the highest SO_3 and lowest Na_2O concentrations (12.0 wt% Na_2O, 1.5 wt% SO_3) among the glasses selected for IDF Phase 1 testing. This glass also contains the highest lithium concentration of 4.37 wt% Li_2O.
- IDF4-A15 and IDF5-A20, based on ORPLA15 and ORPLA20, respectively, are two glasses with high alkali content (24.0 wt% Na_2O, 0.5 wt% K_2O) which have been used in melter tests at the VSL [51, 52]. These compositions meet all of the WTP contract specifications for LAW glass. These glasses have the second highest sodium concentration (after IDF1-B2) as can be seen in Table 2.3.
- IDF6-D6 (22.0 wt% Na_2O, 0.2 wt% K_2O, 1.2 wt% SO_3) was selected from glasses with intermediate sodium content where waste sodium loading is decreased to accommodate

higher sulfate content. The alumina content also is high in this glass (10.1 wt% Al_2O_3) with Al/Si atomic ratio close to $^1/_3$ (see Table 2.3).

- IDF7-E12, based on ORPLE12 (16.0 wt% Na_2O, 0.6 wt% K_2O, 1.5 wt% SO_3) was selected from glasses that could accommodate the highest SO_3 concentration of 1.5 wt%. This glass contains 2.5 wt% Li_2O to improve sulfate solubility. This glass was selected for the full suite of SPFT testing and PCT-B.
- IDF8-A125 based on LAWA125 (20.0 wt% Na_2O, 4.2 wt% K_2O) was selected from high alkali-high potassium glasses with VHT alteration rate and K-3 refractory corrosion neck loss well within the WTP limits. This is a glass with one of the lowest combined alumina and zirconia contents (5.64 wt% Al_2O_3 and 2.91 wt% ZrO_2), but high silica content (42.81 wt% SiO_2) as evident in Figures 2.4 and 2.5.
- IDF9-A187 (23.0 wt% Na_2O, 0.5 wt% K_2O) was selected from glasses with Na_2O concentrations ranging from 23.0 to 23.5 wt%, but with high VHT alteration rate. This glass, as with IDF6-D6, has high Al_2O_3 content and Al/Si ratio close to $^1/_3$ (see Table 2.3).
- IDF10-Zr6 is based on glass LE4H-Zr6 and contains 9.50 wt% ZrO_2. This glass was formulated by increasing the ZrO_2 concentration in the WTP baseline glass LAWE4H by 6 wt%. This glass was included in the set for PCT-B because higher ZrO_2 decreases VHT alteration rate and K-3 neck corrosion, which makes high zirconia of interest for high waste loading LAW glasses. Tests conducted for WRPS [53] to improve technetium retention in LAW glasses showed that ZrO_2 may be beneficial for this application. Accordingly, this glass was selected for PCT-B because none of the other glasses has such high ZrO_2 concentration. Note that this glass has the lowest alumina content (4.95 wt% Al_2O_3), as evident in Figure 2.4.

Among these IDF Phase 1 glasses for which long-term leach tests were initiated in 2010, glasses IDF9-A187CCC and IDF6-D6CCC showed resumption at the earliest, with both showing the formation of analcime and gobbinsite in the alteration products [49]. As noted above, these two glasses have the highest Al_2O_3 content and Al/Si ratio very close to $^1/_3$ (Table 2.3). Zirconium is also relatively low in these two glasses, and in IDF8-A125CCC, which also showed analcime formation in long term leach test results, as reported earlier [49].

For the Phase 2 IDF glasses, seven were selected from the high-alkali region:

- IDF11-G27, based on ORPLG27 (21.0 wt% Na_2O, 5.8 wt% K_2O); this glass has one of the highest alkali oxide concentrations among all of the glasses selected for testing.
- IDF12-A38, based on ORPLA38-1 (24.0 wt% Na_2O, 0.5 wt% K_2O) includes V_2O_5 as an additive for high alkalis glasses to accommodate higher concentrations of SO_3 (0.8 wt%).
- IDF13-A51 based on ORPLA51 (24.0 wt% Na_2O, 0.5 wt% K_2O) investigates the effect of higher TiO_2 concentration.

- IDF14-A59 (24.0 wt% Na_2O, 0.5 wt% K_2O) is a new formulation prepared for the IDF Phase 2 tests; it is based on ORPLA51 but at lower Cl and SO_3 concentrations. Comparison of the long term PCT responses for IDF13-A51 and IDF14-A59 can therefore show the effect of Cl and SO_3 concentrations.
- IDF15-A57 (24.0 wt% Na_2O, 0.5 wt% K_2O) is also a new formulation prepared for the IDF Phase 2 tests. This glass is based on ORPLA57 and, as with the previous two glasses, was formulated with high alumina, titania, and zinc to control K-3 corrosion in high alkali glasses without adding Cr_2O_3. IDF15-A57 contains 10.65 wt% Al_2O_3, 3.0 wt% TiO_2, 4.0 wt% ZnO, but no MgO.
- IDF16-A58 is based on ORPLA58 (24.0 wt% Na_2O, 0.5 wt% K_2O) and is similar in composition to the previous four glasses (10.65 wt% Al_2O_3, 3.0 wt% TiO_2, 3 .0 wt% ZnO), but without CaO.
- IDF17-A60 is based on ORPLA20 with high Na_2O content, but with Cl decreased to 0.1 wt% and SO_3 decreased to 0.3 wt%. In this way, the results from PCT-B of this glass can be compared to those from ORPLA20 because the alkali content in both are fixed at 24.0 wt% Na_2O and 0.53 wt% K_2O.

Three Phase 2 glasses were included to fill the composition gap amongst the lower Na_2O glasses.

- IDF18-A161, based on LAWA161, which was the enhanced formulation for LAW from Tank AN-105 when the waste definition included a higher chlorine content. As a result, the formulation was designed at 20.66 wt% Na_2O and includes 1.17 wt% Cl. This formulation was further tested in a melter at progressively increasing sulfate levels up to 1.10 wt% SO_3 without the formation of secondary sulfate phases [54]. It is also a low zirconium glass (Figure 2.5).
- IDF19-C100 is based on LAWC100 (for Tank AN-102). This formulation is close to LAWA161 in composition but is higher in SO_3 content (1.2 wt%) and lower in Cl content (0.65 wt%). Among the IDF glasses selected for testing, this glass has the highest boron content (Figure 2.7).
- IDF20-F6 is based on ORPLF6, an enhanced formulation for LAW from Tank AZ-101 for which a sodium loading of 13.0 wt% Na_2O would require a sulfate loading of 2.09 wt% SO_3 based on the waste composition [52]. The selected formulation at 13 wt% Na_2O was prepared with a sulfate content of 1.25 wt% SO_3 since that is the sulfate content that was previously evaluated in sulfate oversaturation tests.

All of the glass formulations were fabricated in batches that produced 500 g of glass, which was sufficient to cover all of the planned testing at the VSL. All samples were subjected to canister centerline cooling (CCC) heat treatment [55]. The glasses were analyzed by both X-ray fluorescence spectroscopy (XRF) and direct current plasma - atomic emission spectroscopy

(DCP-AES) after acid dissolution to confirm their composition prior to moving forward with PCT-B and VHT. Details of the preparation and analyses can be found in previous reports [14, 49].

SECTION 3.0
LONG-TERM PCT-B DATA

Long-term PCTs were initiated on ten high waste loading Phase 1 glasses under a test program for WRPS in 2010 [14]. Although funding for that program ended in 2011, most of the long-term PCTs were maintained at VSL's expense and then continued under the 2015 Phase 2 of the IDF program. Also in Phase 2, tests on ten additional glasses were initiated. A summary of the test conditions for these twenty glasses is provided in Table 3.1. This section provides an update on the data for these 20 glasses. These long-term tests were subjected to additional leachate sampling and analysis in order to bring the data set up-to-date. In addition, samples of reacted glass were recovered from selected test vessels for analysis of the secondary phases that have developed [49]. Selected tests are being continued (maintenance, sampling, and analysis) in order to further extend the data set to yet longer times. Note that in the figures presented in association with the discussion below, the sample label is shortened and does not include the "-" separating the IDF number and the original glass code, nor the suffix "CCC," which is part of the sample ID and which denotes the heat treatment that has been imposed on all IDF samples tested herein. It is also noted that ANL-LRM is the PCT reference glass that has undergone PCT-A round robin testing [56]; that glass was tested without receiving the CCC heat treatment.

The product consistency test (PCT; ASTM C1285) [57] is used to evaluate the relative chemical durability of glasses by measuring the concentrations of the chemical species released from 100-200 mesh crushed glass (75-149 μm) to the test solution (de-ionized water in this case). PCT-A (90ºC, 2000 m^{-1} and 7-day) had been performed previously on most of the selected LAW glasses in standard 304L stainless steel leach vessels of 60 mL. PCT-B conducted in the present work used leach vessels of 150 mL capacity (also 304L stainless steel). These vessels have a bottom plug and a top plug assembly that screw on to each end permitting regular leachate sampling through a top septum without breaking the seal of the vessel, and, if needed, sampling of the glass by dismounting the bottom plug.

The PCT-B was performed in triplicate on all of the glasses [14, 49] in parallel with the ANL-LRM reference glass which was included in each test set. For S/V of 2000 m^{-1}, 10 g of glass powder in 100 ml of deionized water is used per vessel; in PCT-B at the higher S/V value (20,000 m^{-1}), 40 g of glass powder is placed in 40 ml of deionized water. All 20 glasses have been tested at 90°C and the high S/V value (20,000 m^{-1}); this was selected in order to investigate the secondary phases that are formed as early as possible. The tests were divided into four sub-sets to keep the immersion sets at a manageable size of 20 vessels (five glass tests in triplicate, plus three standard glasses and two blanks). The sampling protocol consisted of removing an aliquot of 4 ml of the leachate at 7, 28, 56, 120, 181, 270, 365, and 547 days, and yearly thereafter; the solution that is removed for analysis is replaced with 4 ml of deionized water. In addition to the effects of glass composition at 90ºC and S/V of 20,000 m^{-1}, variations in test

temperature (40°C and 90°C) and S/V (2000 m^{-1} and 20,000 m^{-1}) are represented in the dataset for Phase 1 IDF glasses. The data for the Phase 1 glasses now extend to seven years at S/V of 2000 m^{-1}; Phase 2 glasses (90°C and S/V of 20,000 m^{-1}) just passed two years of testing.

3.1 Long-Term PCT-B at 90°C and S/V 20,000 m^{-1}

3.1.1 IDF Phase 1 Data Set

As reported previously [49], the PCT-B at 90°C and S/V 20,000 m^{-1} was performed on the ten Phase 1 glasses and leachate sampling and analysis were performed over 272 days with the exception of three glasses that reached leach rate resumption during that time. This resumption led to normalized releases in excess of 400 g/L (boron normalized release measured at 652, 414, and 423 g/L for IDF6-D6CCC, IDF7-E12CCC and IDF9-A187CCC, respectively). For these three glasses, the leachate was difficult to collect after six months of testing because the solids had agglomerated into a gel and therefore the tests were terminated early. As shown in Figure 3.1, these three glasses show early resumption (shortly after 56 days for IDF9-A187CCC and IDF6-D6CCC and after 120 days for IDF7-E12CCC). The rise in leach rate is sharpest in IDF7-E12CCC with a 60-fold increase between 120 and 180 days. The rates increase by factors of 8 and 5, respectively, for IDF6-D6CCC and IDF9-A187CCC. Similar resumptions occur at later times, between 3 and 6 months, for IDF1-B2CCC and IDF4-A15CCC. Glass IDF8-A125CCC showed noticeably higher leaching in the early samplings (at 7, 28, and 56 days) but did not show such dramatic resumption over the test duration investigated. No new data were collected on these glasses but the results are combined here for comparison to other results presented below. As pointed out earlier, the glasses that showed resumption early have the lowest zirconia, as well as the highest Al_2O_3 contents and Al/Si ratio very close to 1/3. Sampling of the reacted glass samples showed heavy formation of analcime and gobbinsite in the alteration products [49].

The reference glass ANL-LRM also reached resumption with agglomeration at 180 days and those tests were also terminated at that point in the IDF Phase 1 tests.

3.1.2 IDF Phase 2 Data Set

The leachate sampling duration for the ten Phase 2 glasses has now reached two years. The results from sampling of the two PCT sets (designated ILHC and ILHD) since immersion are summarized in Table 3.2 and the normalized boron releases are shown in Figure 3.2; plots of the results for other components are provided in the Appendix. Glass IDF18-A161CCC was the first to reach resumption with a sharp increase in normalized PCT release at 119 days and exceeded 60% altered glass (685 g/L) at the one-and-a-half-year sampling. However, the boron release seems to have slowed down and sodium (Appendix A) shows a similar low-release rate during the past year. A similar increase was observed at 119 days with IDF19-C100CCC, where

the normalized boron PCT release has plateaued near 50% alteration between 273 and 730 days. As shown in Figures 2.4-2.6, these two glasses have the lowest ZrO_2 content among the Phase 2 glasses, comparable to the Phase 1 glasses IDF9-A187CCC and IDF6-D6CCC. In contrast, resumption started for IDF14-A59CCC and IDF20-F6CCC at later sampling dates (273 and 365 days, respectively) but the boron release continued to rise over the last year. Leachate sampling for IDF14-A59CCC at 730 days shows that all available boron has been released (1003 g/L with 0.7%RSD among triplicates). Next to reach resumption was IDF20-F6CCC, which showed a sharp rise in boron PCT release at 365 days (337 g/L). Later sampling showed a continued rise to 642 g/L at two years. Note that IDF20-F6CCC showed the lowest PCT-B release in early sampling, which is consistent with this glass having the lowest alkali concentration (it is the only Phase 2 glass that contains lithium). The rise in leach rate is quite sharp, with the leach rate remaining below 0.1 g/m^2/day before resumption and increasing to ~3 g/m^2/day at resumption for all four of these glasses. The reference glass ANL-LRM2 also reached resumption around the 1-year sampling with excellent agreement between both sets of triplicates from sets ILHC and ILHD. The reason for the slight drop in boron release observed in Figure 3.2 for glasses IDF18-A161CCC and the two ANL-LRM reference glasses is not clear but it has been often observed with glasses at the most advanced stage of leaching, well after resumption occurred. Since, at that point, most of the boron in the glass has been released, some of the drop may be due to the 10% dilution resulting from leachate replacement after sampling; however, the drop is greater than could be explained by that effect alone. At such large extents of alteration, most of the sample has converted into a gelled mass, which might retain some of the leached constituents

In view of the leaching results at one-and-a-half-years and in anticipation of the present report, a small amount of the altered glass (0.25 to 0.33 g of out of 40 g per vessel) was removed at that time from one of the triplicate vessels for glasses IDF14-A59CCC, IDF18-A181CCC, IDF19-C100CCC, IDF20-F6CCC, and the reference glass ANL-LRM2 in set ILHD. Leaching results at the following two-year-sampling was not affected, as is evident from the good agreement between the triplicate sampling solutions (see %RSD in the last page of Appendix A).

Finally, both IDF15-A57CCC and IDF13-A51CCC have reached about 20% of glass alteration (244 and 197 g/L boron normalized release, respectively) at 730 days; they also appear to have reached resumption but show a much slower rate of alteration (~0.5 g/m^2/day) as compared to the glasses discussed above.

3.2 Long-Term PCT-B at 90°C and S/V 2000 m^{-1}

The results from the PCT-B at 90°C and S/V 2000 m^{-1} (IDF Phase 1 glasses only) show a similar trend in leach rate to those observed above at high S/V, but they occur at longer times and in a slightly different order (Figure 3.3; note that at this S/V a normalized boron concentration of 100 g/L corresponds to 100% of the boron content in the glass in solution). Over the last six years of the total of seven years of testing, six of the ten glasses have exhibited elevated rates indicative of resumption. First was IDF9-A187CCC, followed by IDF6-D6CCC

(shortly after 365 and 545 days, respectively). For these two glasses, the order is the same as in the respective higher S/V tests. Resumption was observed next with IDF8-A125CCC, between 720 and 1800 days, but the alteration rate is not as high. For IDF7-E12CCC, resumption occurred at 1200 days with a sharp rise in rate. Resumption of IDF4-A15CCC was observed between 1200 and 1800 days and is still on-going although the rise in alteration rate appears to have slowed down in the last two samplings. Finally, glass IDF3-F7CCC reached resumption with a sharp rise in the last year of sampling. As noted in Figure 3.3, tests for IDF9-A187CCC and IDF6-D6CCC have been terminated and the solid phases collected and analyzed [49]. Small amounts of the altered glass were removed from one of the triplicate vessels from tests IDF8-A125CCC, IDF7-E12CCC, and IDF4-A15CCC, and their analyses were also reported earlier [49]. These, along with IDF3-F7CCC, which has now reached resumption, will be sampled for later analyses to complement findings summarized in Section 4. IDF3-F7CCC was the glass with the lowest normalized release during the previous years; it had reached resumption with a sharp increase of leaching to 47 g/L normalized boron release at year-6 sampling. It is now nearly 90% reacted based on normalized PCT boron release.

As of the last 2017 sampling, IDF5-A20CCC nearly doubled its boron normalized release between each of the last two-yearly samplings (from 8.2 g/L at year 5 to 14.5 g/L at year 6 and 23.5 g/L at year 7), indicative of nearing resumption. Similar observations of nearing resumption are made on IDF1-B2CCC, which has the highest sodium and lowest boron contents (Figure 2.7): boron normalized release doubled from 7.7 to 14.8 g/L in the past year. A small rise in boron normalized release is seen with IDF2-G9CCC, the high potassium glass which appears to be the most durable among this series of high alkali glasses (see Table 2.3). The lowest alteration is observed for the high zirconia glass IDF10-Zr6CCC with lower alkali content (see Table 2.3), which remained near 6% altered glass (boron normalized release of 5.6 to 6.4 g/L) in the last eleven samplings.

The ANL-LRM reference glass [56] continues to show a consistently high rate of alteration, with a higher rise at the latest sampling, with good reproducibility between replicates (now at 25 and 28 g/L boron normalized release, with 0.4%RSD and 0.2%RSD for the two triplicate datasets).

3.3 Long-Term PCT-B at 40°C and S/V 2000 m^{-1}

At the lower test temperature of 40°C, all ten Phase 1 glasses and the ANL-LRM2 reference glass show much less alteration and none of the glasses have reached resumption over the period of testing, as shown in Figure 3.4. Based on normalized boron release, for nine of the glasses, less than 0.5% to 3% of the glass has reacted, all remaining stable over the last three years. Normalized PCT releases and pH measured at room temperature for glass IDF8-A125CCC at 40°C and 90°C are shown in Figures 3.5 and 3.6, respectively. At 40°C, 10 to 11% of the glass has reacted at 900 days and the reaction appears to have stabilized at this level after 2541 days as of the latest sampling. As shown in Figure 3.5, the normalized releases for the two

alkalis follow the same trend but sodium shows a small deviation from congruence with boron (~8.6 g/L on average over the last 6 years) and potassium is found at only a third of the boron release. Although showing much greater alteration at 90°C (Figure 3.6), similarities can be seen between the leaching curves at 40°C and 90°C. Sampling of the solid phases developed on the glasses from both test conditions is scheduled for the future to identify similarities and differences in the phases that have developed.

SECTION 4.0
SECONDARY PHASE ANALYSIS OF IDF PHASE 2 PCT-B SAMPLES

Samples of altered glass were collected from selected ongoing PCT-Bs and analyzed for secondary phases. The results are provided in Tables 4.1 and 4.2. In the present work, glasses were sampled from PCTs that had shown resumption in the past year but none of the vessels from the triplicate sets were sacrificed. A small amount of the altered glass was removed from one of the triplicate vessels (which was then so identified) and the test was continued. Sampling was done in this manner to allow for the possibility that phases developed at the glass surface would be insufficiently crystallized for characterization and, therefore, later sampling would be required. Only 0.25 to 0.33 g of sample was taken out of a total 40 g per vessel (i.e., less than 1%) from the following PCTs, as described in Table 4.2:

- Test ILHC, sample IDF14-A59CCC
- Test ILHC, sample ANL-LRM2
- Test ILHD, sample IDF18-A161CCC
- Test ILHD, sample IDF19-C100CCC
- Test ILHD, sample IDF20-F6CCC
- Test ILHD, sample ANL-LRM2.

The selected altered glass samples were collected after 18 months of PCT at 90°C and 20,000 m^{-1} S/V. The powder was rinsed and dried prior to preparation for analysis by Scanning Electron Microscopy/Energy Dispersive X-ray Spectroscopy (SEM/EDS) and X-ray Diffraction (XRD).

For XRD analysis, dried samples of altered glasses were crushed and then deposited onto a sample holder. This was necessary to avoid preferential crystal orientation, which would hinder phase identification by XRD. The amount collected for XRD was very small for some of the samples (due to agglomeration of the glass sample in the leach vessel) and care was taken to avoid loss of material during grinding. The XRD powder patterns were collected using a Thermo ARL X'tra θ-θ X-ray diffractometer with copper Kα X-rays. Data were gathered over a 5 to 80° 2θ range, where the interval between data points was 0.02° and the collection time per data point was 4 seconds. Identification of the crystalline phases in the samples was performed by matching diffraction features in the powder patterns to the International Centre for Diffraction Data (ICDD) databases using JADE9 search/match routines. In previous analyses of altered samples from glasses in this inventory that have been subjected to long-term PCT, typical phases have included nontronite, saponite, smectites (phyllosilicate mineral species), phillipsite, zeolites, analcime (tectosilicate mineral species), etc. [14, 49].

SEM/EDS was performed on a JEOL JSM-5910LV electron microscope to characterize the microstructure developed at the glass/leachant interface and to analyze the crystalline phases present on the glass surface. A few milligrams of each sample were mounted on a ½-inch metal cylinder and coated with carbon. Typical magnifications used ranged from 25× to 8,000×. Both backscattered and secondary electron imaging were used; working conditions for this purpose were 20 kV accelerating voltage, 0.45 nano-amp probe current, 60 seconds X-ray collection time, 10 mm working distance, and 20 micron objective aperture.

Observations regarding the secondary phases in the previous samples [14, 49] are collected in Table 4.1 and results from the present samples are summarized in Table 4.2 and discussed below.

The XRD pattern for IDF14-A59CCC (Figures 4.1) includes the broad pattern characteristic of glass, which is the most visible feature, and shows some crystal content, as is evident from the sharp peaks in the XRD spectrum. The XRD powder pattern that best matches the crystalline phase is the zeolite phillipsite $(K,Na)_2(Si,Al)_8O_{16}\cdot 4H_2O$. The XRD patterns for the other four glasses are collected together in Figure 4.2. Based on qualitative comparison of peak intensities in the XRD spectra, the crystal content is higher in the other four samples than in IDF14-A59CCC. The zeolite phillipsite $(K,Na)_2(Si,Al)_8O_{16}\cdot 4H_2O$ was identified in all five glass samples, which show XRD peaks at 2θ values of 13°, 18°, 22°, 28°, and 33°. The zeolite pattern is most visible in ANL-LRM2 and IDF18-A161CCC and less so in IDF19-C100CCC and IDF20-F6CCC. Some Analcime (XRD peak at 2θ of 26°) is also detected in ANL-LRM2 but not in any of the other samples.

Other XRD peaks are also visible in IDF18-A161CCC, IDF19-C100CCC, and IDF20-F6CCC, which are best matched by phyllosilicates of the chlorite and smectite groups, as given in the lower section of Figure 4.2. Aliettite ($Ca_{0.9}Mg_6(Si,Al)_8O_{22}(OH)_4\cdot 4(H_2O)$), beidellite ($Na_{0.3}Al_2(Si,Al)_4O_{10}(OH)_2\cdot 2(H_2O)$), and swinefordite ($Ca_{0.1}(Li,Al)_3Si_4O_{10}(OH)_2\cdot 2(H_2O)$ are three possible smectites that are present in these samples. Phyllosilicates are so named because their crystal structures are comprised of silicate sheets, with alternating tri-octahedral sheets that contain divalent cations (Mg^{2+}, Fe^{2+}, Zn^{2+}) or with alternating di-octahedral sheets that contain trivalent cations (Al^{3+}, Fe^{3+}, …). Exchangeable cations (Na^+, K^+, and Li^+) as well as water molecules may also be found between layers. These also play the role of charge balance to compensate for the inclusion of charge deficient cations in the silicate sheet structure. Cation substitutions in the layered structure of the clay produce ranges of d-spacings between sets of atomic planes and, consequently, broaden the corresponding diffraction peaks; this is generally evident in the XRD peaks around 2θ of 62-65°. Such broad peaks are seen mostly in IDF19-C100CCC and IDF20-F6CCC. An illustration showing lithium in structural and interlayer positions is shown in Appendix B, which could be the case for the phase swinefordite $(Ca_{0.1}(Li,Al)_3Si_4O_{10}(OH)_2\cdot 2(H_2O)$ present in IDF20-F6CCC, the only glass with lithium in this PCT set.

SEM/EDS observations are provided below with a discussion of the results, supplemented by the above XRD data for best identification of the phases observed on the altered glass samples.

Glass IDF14-A59CCC (Figure 4.3) appears to be covered by a thin (sub-micron) layer, which is often found spalled or cracked. The dominant crystal is a euhedral acicular aluminosilicate, which forms small clusters at the glass surface. SEM/EDS analyses taken over two dozen locations average to the formula $(Na_{6.7}K_{0.1}Mg_{0.4}Ca_{0.2}Ti_{0.8}Zn_{0.4})Al_2Si_7O_{24}$ for the zeolite observed. The ratio of Si/Al remained very constant at 3.5 in this zeolite but variations in Mg, Ti, and Zn are large (~30% relative). From the crystal morphology (Figure 4.3h), it seems that phyllosilicates are present, but EDS analysis did not confirm their presence.

Glasses IDF18-A161CCC (Figure 4.4) and IDF19-C100CCC (Figure 4.5), which underwent earliest resumption, both show the formation of tectosilicates, with radial fibrous sphere morphology in IDF19-C100CCC that can be identified as phillipsite (average composition $Na_{3.1}Ca_{0.9}Al_{3.2}Si_{10.2}O_{32}$)[58]. For both glasses, the solids appear to have clustered, probably as a result of adhesion of the glass grains via the gel layers. In IDF18-A161CCC, crystals with bladed rosette morphology were observed (Figures 4.4 e, f, and g). Both the morphology and EDS analyses match the feldspar albite ($NaAlSi_3O_8$ with traces of potassium and iron). The phase appears compositionally close to albites, but probably also contains some H_2O; however, because any possible hydration cannot be measured by EDS, the identification can only be tentative. The $[SiO_4]^{4-}$ and $[AlO_4]^{5-}$ building blocks of a zeolite such as the phillipsite identified by XRD could also be combined to approach the formula indicated by EDS analysis (+ some H_2O). In IDF19-C100CCC, radiating prisms of phillipsite are clearly seen (Figure 4.5-d) forming botryoidal clusters when observed in another direction (Figure 4.5-e). Series of EDS analyses taken throughout the sample showing varying amounts of Ca, Zn, and Zr yield the average formula $(Na_6CaFe_{0.1}Zn_{0.3}Zr)Al_3Si_{10}O_{24}$. The morphology that was previously identified in published studies on the alteration products of magmatic minerals [58] supports the identification of the phase present in the alteration products of IDF19-C100CCC as a phillipsite. The morphology that is shown in Figure 4.5-e in the red square inset matches closely that previously reported and identified as phillipsite [58], one of the zeolites formed during sub-solidus hydrothermal alteration (<150 °C) under alkaline conditions [58, 59] of a basaltic glass.

An acicular aluminosilicate that forms small fibrous clusters, as was seen in IDF14-A59CCC, was also detected in IDF20-F6CCC. However, a more visible crystal, seen in Figure 4.6-d, matches the morphology and composition in EDS of a calcium-vanadium silicate (Figure 4.7), which could be identified as the phyllosilicate cavansite $Ca(VO)Si_4O_{10}(H_2O)_4$. Although not previously detected in alteration products of Hanford LAW long-term PCT samples, vanadium containing phases have been seen on the surface of VHT coupons [60]. Crystals of zinc silicate could be matched by their morphology and composition to $Zn_4Si_2O_7(OH)_2{\cdot}H_2O$ (Figure 4.8), possibly as the sorosilicate hemimorphite. However, attempts to refit the XRD

spectrum did not match either of these two phases, which are probably not abundant enough to show sufficiently detectable XRD peaks.

Evaluation of the two ANL-LRM2 reference glass samples showed agglomerated glass grains with large spalled layers (Figures 4.9). Crystals of three main morphologies can be seen: sub-euhedral, elongated and reticulated crystals, and prismatic columns and ball-shaped aggregates. The EDS analyzed compositions of all of these are consistent with the formula $(Na_{3.7}K_{0.1}Mg_{0.2}Ca_{0.6}Fe_{0.1}Zn_{0.41}Zr_{0.3})Al_{1.5}Si_{4.8}O_{16}$, with variations in sodium (3.4 to 4.3), aluminum (1.2 to 1.6), and calcium (0.2 to 1.6).

As was the case with Phase 1 glasses that have reached resumption, the phases identified in the Phase 2 leached glass samples are tecto- or sorosilicates, as characterized in XRD by well-defined sharp diffraction peaks. In SEM, these are structures that developed above the glass surface. In these Phase 2 glasses, phyllosilicates, if present, could not be identified. In contrast, phyllosilicates were identified in Phase 1 glasses, even when alteration remained low, together with tectosilicates for glasses that underwent resumption. Sampling of the other IDF Phase 2 glasses that have not reached resumption has been reserved for future years in order to allow longer time for the alteration products to develop sufficiently and crystallization to mature to more identifiable forms. Among the five glasses sampled so far, none have shown the presence of the dodecahedral crystals characteristic of analcime, which are typically ~50 μm in size and easily identified by SEM. Furthermore, very small amounts of phyllosilicates have been observed. This may be attributable to the relatively short durations of the tests. Future sampling of Phase 1 and Phase 2 glasses, including some repeat sampling from PCTs that have already reached resumption, will complement the present results and should assist in better identification of the crystalline phases.

SECTION 5.0
SUMMARY AND CONCLUSIONS

This report provides results of work performed to collect information on the corrosion behavior of LAW glasses to support the IDF PA. In addition to the development of the baseline operating envelope for the WTP, since 2003, VSL has been developing a wide range of LAW formulations that achieve considerably higher waste loadings than the WTP baseline formulations. As a result, the range of glass compositions that may be produced at the WTP is expanding toward higher sodium and sulfate contents and new glass forming additives, and this type of composition range expansion is likely to continue through the life of the project. In an initial effort (Phase 1) started to encompass the composition range expected to be disposed at the IDF, a total of 10 Phase 1 glasses were selected for this composition expansion [14]. The selection was based on an analysis of the compositions and properties of the large number of LAW glasses that have been developed for the WTP at VSL. Those glasses were subjected to testing using the long-term PCT-B and selected glasses were tested according to the SPFT method to determine rate law parameters. The Phase 1 program ended in 2011 but most long-term PCTs were maintained at VSL's expense. Work conducted under Phase 2 offered the opportunity to report the leachate data from those tests that were continued and to characterize the alteration phases [49]. A second objective of the Phase 2 work was to extend the Phase 1 study by adding ten new high waste loading glasses in order to further span the expanded glass composition range, taking into consideration more recent high waste loading compositions that have been developed for ORP at VSL. The Phase 1 and Phase 2 glasses include compositions that are bounding with respect to performance on the WTP leach test specifications (PCT and VHT), that are higher in waste loading than the baseline WTP glasses, and that include variations in significant minor components such as sulfate and chlorine, as well as glass constituents that are not present in the baseline glasses. The Phase 2 series also includes one glass (IDF15-A57CCC) with a VHT response that exceeds the WTP contract limit.

Many of the long-term PCT-Bs initiated in Phase 1 and all of the long-term PCT-Bs initiated on the ten Phase 2 glasses are ongoing and yet longer-term data will be collected. The most recent data show that among the ten Phase 1 glasses tested at 90°C and S/V 2000 m^{-1}, six are now over 50% reacted and one (IDF5-A20) is showing a rising leach rate in the past year. However, the two high-alkali bounding glasses, IDF1-B2 and IDF2-G9, and the high zirconia glass IDF10-Zr6 are still showing low leach rates: 15%, 8%, and 6% reacted, respectively. In contrast, no change has been observed for the Phase 1 glasses tested at 40°C and S/V 2000 m^{-1}. Among the Phase 2 glasses tested at 90°C and S/V of 20,000 m^{-1}, two reached resumption within the first six months, two others and the reference glass ANL-LRM2 reached resumption within the first year, and two more reached resumption in the past year. These are generally low-zirconia glasses (less than 2 mole% Zr) with high alumina (above 9 mole% Al). All glasses that have reached resumption at the earliest time in each set of tests are found in the lower section of Figure 2.4 with low Zr concentrations of about 2 mol% or less. Since these are not the glasses

with the highest alkali content, high-alkali alone is not the determining factor in the relatively rapid alteration.

XRD and SEM/EDS evaluation of solid samples taken from the leach tests of Phase 2 glasses at 90°C and 20,000 m^{-1} S/V permitted identification of phases present at the glass surface, which, for the most part, are tecto- and sorosilicates. The morphology of some of these zeolite crystals had not been observed before in Hanford LAW glass alteration products (long-term PCT or VHT). However, some phases of similar morphology were previously identified in alteration of basaltic glass formed from volcanic activity 15 to 20 million years ago. The alteration in these natural analogues results in the formation of various zeolites during sub-solidus hydrothermal alteration (<150 °C) under alkaline conditions [58, 59] and provides a good resource for identification of crystal morphologies also observed in the present LAW glass samples.

SECTION 6.0
QUALITY ASSURANCE

This work was conducted under a quality assurance program compliant with the applicable criteria of 10 CFR 830.120; the American Society of Mechanical Engineers (ASME) Nuclear Quality Assurance (NQA)-1-2008 including NQA-1a-2009 Addenda; and DOE Order 414.1D, Quality Assurance. These QA requirements are implemented through a Quality Assurance Project Plan for WRPS work [61] that is conducted at VSL. Test and procedure requirements by which the testing activities are planned and controlled are also defined in this plan. The program is supported by VSL standard operating procedures that were used for this work [62]. This is LAW work and is therefore not subject to the requirements of DOE/RW-0333P, Office of Civilian Waste Management Quality Assurance Requirements and Description (QARD), Revision 20.

SECTION 7.0
REFERENCES

[1] "A Strategy to Conduct an Analysis of the Long-Term Performance of Low-Activity Waste Glass in a Shallow Subsurface Disposal System at Hanford," B.P. McGrail, W.L. Ebert, D.H. Bacon and D.M. Strachan, PNNL-11834, Pacific Northwest National Laboratory, Richland, WA, (1998).

[2] "An International Initiative on Long-Term Behavior of High-Level Nuclear Waste Glass", S. Gin, A. Abdelouas, L.J. Criscenti, W.L. Ebert, K. Ferrand, T. Geisler, M.T. Harrison, Y. Inagaki, S. Mitsui, K.T. Mueller, J.C. Marra, C.G. Pantano, E.M. Pierce, J.V. Ryan, J.M. Schofield, C.I. Steefel and J.D. Vienna,*Materials Today* **16**(6) 243-248 (2013).

[3] "Waste Form Release Data Package for the 2001 Immobilized Low-Activity Waste Performance Assessment," B.P. McGrail, J.P. Icenhower, P.F. Martin, H.T. Schaef, M.J. O'Hara, E.A. Rodriguez, and J.L. Steele, PNNL-13043, Rev. 2, Pacific Northwest National Laboratory, Richland, WA (2001).

[4] Request for Off-Site Services (Technical) Statement of Work, "ILAW Glass Testing for Disposal at IDF, Rev. 1," Requisition #:270768, Washington River Protection *Solutions*, LLC (WRPS), 12/10/14.

[5] "Experimentally Determined Dissolution Kinetics of Na-rich Borosilicate Glasses at Far-From-Equilibrium Conditions: Implications for Transition State Theory," J.P. Icenhower, B.P. McGrail, W.J. Shaw, E.M. Pierce, P. Nachimuthu, D.K. Shuh, E.A. Rodriguez, and J.L. Steele, *Geochimica Cosmochimica Acta* **72**, 2767-2788 (2008).

[6] "Measurement of Kinetic Rate Law Parameters on a Na-Ca-Al Borosilicate Glass for Low-Activity Waste," B.P. McGrail, W.L. Ebert, A.J. Bakel, and D.K. Peeler, *J. Nucl. Mater.* **249**, 175-189 (1997).

[7] "Low-Activity Waste Glass Studies: FY 2000 Summary Report," B.P. McGrail, J.P. Icenhower, P.F. Martin, D.R. Rector, H.T. Schaef, E.A. Rodriguez, and J.L. Steele, PNNL-13381, Pacific Northwest National Laboratory, Richland, WA (2000).

[8] "Laboratory Testing of Bulk Vitrified Low-Activity Waste Forms to Support the 2005 Integrated Disposal Facility Performance Assessment," E.M. Pierce, B.P. McGrail, L.M. Bagaasen, E.A. Rodriguez, D.M. Wellman, K.N. Geiszler, S.R. Baum, L.R. Reed, J.V. Crum, and H.T. Schaef, PNNL-15126, Rev. 2, Pacific Northwest National Laboratory, Richland, WA (2005).

[9] "Kinetic Rate Law Parameter Measurements on Borosilicate Waste Glass: Effect of Temperature, pH, and Solution Composition on Alkali Ion Exchange," E.M. Pierce, B.P. McGrail, J.P. Icenhower, E.A. Rodriguez, J.L. Steele, and S.R. Baum, *American Chemical Society Division of Environmental Chemistry*. American Chemical Society, Philadelphia, PA (2004).

[10] "Waste Form Release Data Package for the 2005 Integrated Disposal Facility Performance Assessment," E.M. Pierce, B.P. McGrail, E.A. Rodriguez, H.T. Schaef, K.P. Saripalli, R.J. Serne, K.M. Krupka, P.F. Martin, S.R. Baum, K.N. Geiszler, L.R. Reed, and W.J. Shaw, PNNL-14805, Pacific Northwest National Laboratory, Richland, WA (2004).

[11] "An Experimental Study of the Dissolution Rates of Simulated Aluminoborosilicate Waste Glasses as a Function of pH and Temperature under Dilute Conditions," E.M. Pierce, E.A. Rodriguez, L.J. Calligan, W.J. Shaw, and B.P. McGrail, *Applied Geochemistry* **23**, 2559-2573 (2008).

[12] "A Strategy to Conduct an Analysis of the Long-Term Performance of Low-Activity Waste Glass in a Shallow Subsurface Disposal System at Hanford," J.J. Neeway, E.M. Pierce, V.L. Freedman, J.V. Ryan, and N.P. Qafoku, PNNL-23503, Rev. 0, Pacific Northwest National Laboratory, Richland, WA (2014).

[13] "Immobilized Low-Activity Waste Glass Release Data Package for the Integrated Disposal Facility Performance Assessment," V.L. Freedman, J.V. Ryan, and D.H. Bacon, PNNL-24615, Draft, Pacific Northwest National Laboratory, Richland, WA, August 2015.

[14] "ILAW Glass Testing for Disposal at IDF: Phase 1 Testing," A.E. Papathanassiu, I.S. Muller, M. Brandys, K. Gilbo, A. Barkatt, I. Joseph and I.L. Pegg, VSL-11R2270-1, Rev. 0, Vitreous State Laboratory, The Catholic University of America, Washington, DC, 6/6/11.

[15] "The Activated Complex in Chemical Reactions," H. Eyring, *J. Chem. Phys.* **3**, 107-114 (1935).

[16] "Thermodynamic and Kinetic Constraints on Reaction Rates among Minerals and Aqueous Solutions. I. Theoretical Considerations," P. Åagaard and H.C. Helgeson, *Am. J. Sci.* **282**, 237-285 (1982).

[17] "A General Rate Equation for Nuclear Waste Glass Corrosion," B. Grambow, *Material Research Symposium Proceedings* **44**, 15-27 (1985).

[18] "Kinetic Ion Exchange Salt Effects on Glass Leaching," X. Feng and I.L. Pegg, *Energy, Environment and Information Management*, Eds. H. Wang, S. Chang, and H. Lee, Argonne, IL, p. 7-9, (1992).

[19] "Effects of Salt Solutions on Glass Dissolution," X. Feng and I.L. Pegg, *Phys. Chem. Glasses*, **35**, 1 (1994).

[20] "A Glass Dissolution Model for the Effects of S/V on Leachate pH," X. Feng and I.L. Pegg, J. *Non-Cryst. Solids*, **175**, 281 (1994).

[21] "Characterization of Alteration Phases on HLW Glasses after 15 Years of PCT Leaching," I.S. Muller, S. Ribet, I.L. Pegg, S. Gin, and P. Frugier, *Ceramic Transactions*, Vol. 176 (2005).

[22] "Long-Term PCT Data for LAW Glasses," I.S. Muller, D.A. McKeown, X. Xie, I.L. Pegg, and I. Joseph, Final Report, VSL-17R4090-1, Rev. 0, Vitreous State Laboratory, The Catholic University of America, Washington, DC, 05/30/17.

[23] "Dissolution and Precipitation Kinetics of Sheet Silicates," K.L. Nagy, *Reviews in Mineralogy and Geochemistry*, **31**, 173-233, Mineralogical Society of America, Chantilly, VA (1995).

[24] "Letter: Simultaneous Precipitation Kinetics of Kaolinite and Gibbsite at 80°C and pH 3," K.L. Nagy, and A.C. Lasaga, *Geochimica et Cosmochimica Acta* **57**, 4329 – 4335 (1993).

[25] "Preliminary Results of Durability Testing with Borosilicate Glass Compositions," M. Adel-Hadadi, R. Adiga, Aa. Barkatt, X. Feng, I.L. Pegg, et al., Tech. Info. Center, Office of Sci. and Tech. Info., USDOE, DOE/NE/44139-34, (1988).

[26] "Compositional Effects on Chemical Durability and Viscosity of Nuclear Waste Glasses – Systematic Studies and Structural Thermodynamic Models," X. Feng, Ph.D. Thesis, The Catholic University of America (1988).

[27] "Leach Rate Excursions in Borosilicate Glasses: Effects of Glass and Leachant Composition," Aa. Barkatt, S.A. Olszowka, W. Sousanpour, M.A. Adel-Hadadi, R. Adiga, Al. Barkatt, G.S. Marbury, and S. Li, Mat. Res. Soc. Symp. Proc., 212, 65 (1991).

[28] "Alteration Layers on Glasses After Long-Term Leaching," A.C. Buechele, S.T.- Lai, and I.L. Pegg, *Ceramic Transactions*, Eds. D.K. Peeler and J.C. Marra, vol. 87, p. 423, American Ceramic Society (1998).

[29] "Compositional Effects on the Long-Term Durability of Nuclear Waste Glasses: A Statistical Approach," S. Ribet, I.S. Muller, I.L. Pegg, S. Gin, and P. Frugier, Mat. Res. Soc. Symp. Proc. Vol. 824 (2004).

[30] "The Long-Term Corrosion and Modeling of Two Simulated Belgian Reference High-Level Waste Glasses – Part II," J. Patyn, P. Van Iseghem, and W. Timmermans, Mat. Res. Symp. Soc. Proc., 176, 299 (1990).

[31] "New Insight into the Residual Rate of Borosilicate Glasses: Effect of S/V and Glass Composition", S. Gin, P. Frugier, P. Jollivet, F. Bruguier, E. Curti, Int. J. Appl. Glass Sci., 4, 371-382 (2013).

[32] "Nuclear Glass Durability: New Insight into Alteration Layer Properties," S. Gin, C. Guittonneau, N. Godon, D. Neff, D. Rebiscoul, M. CabieS. Mostefaoui, J. Phys. Chem. C 115, 18696-18706, (2011).

[32] "An International Initiative on Long-Term Behavior of High-Level Nuclear Waste Glass," S. Gin, A. Abdelouas, L.J. Criscenti, W.L. Ebert, K. Ferrand, T. Geisler, M.T. Harrison, *et al.*, Mater. Today 16, 243–248 (2013).

[34] "Origin and Consequences of Silicate Glass Passivation by Surface Layers", S. Gin, P. Jollivet, M. Fournier, F. Angeli, P. Frugier, T. Charpentier, Nat. Commun., 6 (2015).

[35] "The Fate of Silicon During Glass Corrosion Under Alkaline Conditions: A Mechanistic and Kinetic Study with the International Simple Glass," S. Gin, P. Jollivet, M. Fournier, C. Berthon, Z. Wang, A. Mitroshkov, Z. Zhu, J. V. Ryan, Geochim. Cosmochim. Acta, 151, 68–85 (2015).

[36] "Resumption of Nuclear Glass Alteration: State of the art," M. Fournier, S. Gin, P. Frugier, J. Nucl. Mater., 448, 348–363 (2014).

[37] "Open Scientific Questions About Nuclear Glass Corrosion," S. Gin, Procedia Materials Science, 163-171 (2014).

[38] "Current Understanding and Remaining Challenges in Modeling Long-Term Degradation of Borosilicate Nuclear Waste Glasses," J.D. Vienna, J.V. Ryan, S. Gin, and Y. Inagaki, Int. J. Appl. Glass Sci., 4, 283–294 (2013).

[39] "Contribution of Atom-Probe Tomography to a Better Understanding of Glass Alteration Mechanisms: Application to a Nuclear Glass Specimen Altered 25 years in a Granitic Environment," S. Gin, J.V. Ryan, D.K. Schreiber, J. Neeway, and M. Cabie, Chem. Geol. 349, 99–109 (2013).

[40] "Effect of Composition on the Short-Term and Long-Term Dissolution Rates of Ten Borosilicate Glasses of Increasing Complexity from 3 to 30 Oxides", S. Gin, X. Beaudoux, F. Angeli, C. Jegou, N. Godon, J. Non-Cryst. Solids, 358, 2559–2570 (2012).

[41] "Development of the Vitrification Compositional Envelope to Support Complex-Wide Application of MAWS Technology," I.S. Muller, H. Gan, A.C. Buechele, S.T. Lai, and I.L. Pegg, DOE/CH-9601, September 1996.

[42] "Alteration Phases on High Sodium Waste Glasses after Short- and Long-Term Hydration," A.C. Buechele, S.-T. Lai, and I.L. Pegg, *Ceramic Transactions*, vol. 107, p. 251 (2000).

[43] "Waste Loading Enhancements for Hanford LAW Glasses," I.S. Muller, K.S. Matlack, H. Gan, I. Joseph, and I.L. Pegg, Final Report, VSL-10R1790-1, Rev. 0, Vitreous State Laboratory, The Catholic University of America, Washington, DC, 12/01/10.

[44] "Improved High-Alkali Low-Activity Waste Formulations," I.S. Muller, M. Chaudhuri, H. Gan, A. Buechele, X. Xie, I.L. Pegg, and I. Joseph, Final Report, VSL-15R3290-1, Rev. 0, Vitreous State Laboratory, The Catholic University of America, Washington, DC, 08/12/15.

[45] "Enhanced LAW Glass Property-Composition Models – Phase 2," I.S. Muller, K. Gilbo, I. Joseph, and I.L. Pegg, Final Report, VSL-14R3050-1, Rev. 0, Vitreous State Laboratory, The Catholic University of America, Washington, DC, 8/29/14.

[46] "FY2016 ILAW Glass SPFT Testing for Disposal at IDF," A.E. Papathanassiu, C. Viragh, I.S. Muller, and I.L. Pegg, VSL-17R3860-1, Rev. 0, Vitreous State Laboratory, The Catholic University of America, Washington, DC, 7/12/17.

[47] "FY2016 ILAW Glass Corrosion Testing with the Single-Pass Flow-Through Method," J.J. Neeway, R.M Asmussen, B.P. Parruzot, E.A. Cordova, B.D. Williams, I.L. Leavy, J.R. Stephenson, and E.M. Mcelroy, PNNL-26169, RPT-IGTP-013 Rev. 0.0, Pacific Northwest National Laboratory, Richland, WA (2017).

[48] "Immobilized Low-Activity Waste Glass Release Data package for the Integrated Disposal Facility Performance Assessment," V.L. Freedman, J.V. Ryan and D.H. Bacon, PNNL-24615, RPT-IGTP-005, Rev. 0, Pacific Northwest National Laboratory, Richland, WA, September, 2015.

[49] "FY15 ILAW Glass Testing for Disposal at IDF", I.S. Muller, and I.L. Pegg, VSL-15R3790-1, Rev. 0, Vitreous State Laboratory, The Catholic University of America, Washington, DC, 4/15/16.

[50] "FY2016 update on ILAW Glass Testing for Disposal at IDF", I.S. Muller, and I.L. Pegg, VSL-16S4170-1, Rev. 0, Vitreous State Laboratory, The Catholic University of America, Washington, DC, 2/1/17.

[51] "Enhanced LAW Glass Formulation Testing," K.S. Matlack, I. Joseph, W. Gong, I.S. Muller, and I.L. Pegg, Final Report, VSL-07R1130-1, Rev. 0, Vitreous State Laboratory, The Catholic University of America, Washington, DC, 10/05/07.

[52] "Glass Formulation Development and DM10 Melter Testing with ORP LAW Glasses," K.S. Matlack, I. Joseph, W. Gong, I.S. Muller, and I.L. Pegg, Final Report, VSL-09R1510-2, Rev. 0, Vitreous State Laboratory, The Catholic University of America, Washington, DC, 6/12/09.

[53] "Improving Technetium Retention in Hanford LAW Glass – Phase 1," K.S. Matlack, I.S. Muller, I. Joseph and I.L. Pegg, Final Report, VSL-10R1920-1, Rev. 0, Vitreous State Laboratory, The Catholic University of America, Washington, DC, 03/19/10.

[54] "Glass Formulation Testing to Increase Sulfate Incorporation," K. S. Matlack, M. Chaudhuri, H. Gan, I.S. Muller, W. Gong, and I.L. Pegg, Final Report, VSL-04R4960-1, Rev. 0, Vitreous State Laboratory, The Catholic University of America, Washington, DC, 2/28/05.

[55] "LAW Container Centerline Cooling Data," RPP-WTP Memorandum, L. Petkus to C. Musick, CCN# 074181, River Protection Project−Waste Treatment Plant, Richland, WA, 10/16/03.

[56] "Round Robin Testing of a Reference Glass for Low-Activity Waste Forms," W.L. Ebert and S.F. Wolf, Department of Energy Report ANL-99/22, Argonne National Laboratory, Argonne, IL (1999).

[57] "Standard Test Methods for Determining Chemical Durability of Nuclear, Hazardous, and Mixed Waste Glasses and Multiphase Glass Ceramics: The Product Consistency Test (PCT)," ASTM C 1285-08, American Society for Testing and Materials, West Conshohocken, PA, 2008.

[58] "Hydrothermal alteration and zeolitization of the Fohberg phonolite, Kaiserstuhl Volcanic Complex, Germany", T. Weisenberger and N. Spürgin, Int J Earth Sci (Geol Rundsch) (2014) 103:2273–2300.

[59] "Zeolites in Alkaline Rocks of the Kaiserstuhl Volcanic Complex, SW Germany – New Microprobe Investigation and the Relationship of Zeolite Mineralogy to the Host Rock" T. Weisenberger and N. Spürgin, Geologica Belgica (2009) 12/1-2: 75-91.

[60] "Enhanced LAW Glass Correlation – Phase 3," I.S. Muller, K. Matlack, I.L. Pegg and I. Joseph," Test Plan, VSL-17R4230-1, Rev. A, Vitreous State Laboratory, The Catholic University of America, Washington, DC, 10/2/17.

[61] "Quality Assurance Project Plan for WRPS Support Activities Conducted by VSL," Vitreous State Laboratory, QAPP-WRPS, Rev. 4, Vitreous State Laboratory, The Catholic University of America, Washington, DC, 9/14/16.

[62] "Master List of Controlled VSL Manuals and Standard Operating Procedures in Use," QA-MLCP, Rev. 155, Vitreous State Laboratory, The Catholic University of America, Washington, DC, 6/19/17.

Table 2.1. Target Compositions of the Ten IDF Phase 1 Glasses (wt%).

Glass	IDF1-B2	IDF2-G9	IDF3-F7	IDF4-A15	IDF5-A20	IDF6-D6	IDF7-E12	IDF8-A125	IDF9-A187	IDF10-Zr6
Al_2O_3	10.00	6.76	8.65	9.45	6.65	10.09	7.58	5.64	10.57	4.95
B_2O_3	7.30	8.51	9.53	8.60	8.74	9.85	9.82	9.55	12.77	11.77
CaO	1.10	2.70	9.77	3.32	3.32	7.89	10.02	1.94	6.47	2.43
Cr_2O_3	0.52	0.59	0.56	0.49	0.50	0.50	0.50	0.02	0.52	0.08
Cs_2O	0.15	-	-	0.14	-	-	0.15	0.18	-	-
Fe_2O_3	1.10	0.20	0.23	0.92	0.19	0.28	0.24	5.39	0.90	6.70
K_2O	0.12	5.76	0.50	0.54	0.53	0.17	0.55	4.21	0.51	0.54
Li_2O	-	-	4.37	-	-	-	2.49	-	-	-
MgO	1.10	0.96	0.98	0.92	0.92	1.00	1.04	1.44	0.90	1.45
MnO_2	0.06	-		-	-	-	-	-	-	-
Na_2O	25.00	21.00	12.00	24.00	24.00	22.00	16.00	20.00	23.00	21.27
NiO	0.04	0.01	-	-	-	0.04	-	-	-	0.01
PbO	-	0.01	-	-	-	0.01	-	-	-	0.01
SiO_2	39.88	40.82	42.38	39.17	42.24	37.14	41.19	42.81	34.70	38.89
SnO_2	1.08	2.84	-	2.73	2.74	-	-	-	1.00	-
TiO_2	-	-	-	-	-	-	-	1.94	-	-
V_2O_5	2.00	-	2.50	-	-	1.96	1.74	-	0.97	-
ZnO	3.65	3.40	2.92	2.43	2.74	2.96	3.21	2.88	2.99	1.50
ZrO_2	5.44	5.68	3.92	5.91	5.96	3.98	3.53	2.91	2.99	9.50
Cl	0.11	0.23	0.01	0.68	0.67	0.35	0.02	0.22	0.64	0.20
F	0.49	0.09	0.08	0.00	0.00	0.18	0.20	0.32	-	0.08
P_2O_5	0.23	0.14	0.04	-	-	0.30	0.12	0.08	-	0.12
SO_3	0.52	0.20	1.50	0.60	0.70	1.20	1.50	0.37	0.95	0.41
Re_2O_7	0.10	0.10	0.10	0.10	0.10	0.10	0.10	0.10	0.10	0.10
SUM	100.0	100.0	100.0	100.0	100.0	100.0	100.0	100.0	100.0	100.0

- Empty data field

Table 2.2. Target Compositions of the Ten IDF Phase 2 Glasses (wt%).

Glass	IDF11-G27	IDF12-A38	IDF13-A51	IDF14-A59	IDF15-A57	IDF16-A58	IDF17-A60	IDF18-A161	IDF19-C100	IDF20-F6
Al_2O_3	6.03	6.94	10.15	10.31	10.65	10.65	6.75	10.04	10.16	8.48
B_2O_3	7.92	8.21	8.02	8.15	8.05	8.75	8.87	13.51	13.68	9.36
CaO	2.69	3.12	1.00	1.02	1.50	-	3.37	7.90	8.02	9.58
Cr_2O_3	0.59	0.49	0.02	0.02	0.02	0.02	0.51	0.02	0.02	0.56
Cs_2O	-	-	-	-	-	-	-	0.15	-	-
Fe_2O_3	0.28	0.26	0.19	0.19	0.05	0.25	0.19	0.99	1.00	0.29
K_2O	5.75	0.53	0.53	0.53	0.53	0.53	0.53	0.44	0.15	0.54
Li_2O	-	-	-	-	-	-	-	-	-	3.45
MgO	0.44	0.98	1.93	1.96	-	1.55	0.93	0.99	1.00	0.97
Na_2O	21.00	24.00	24.00	24.00	24.00	24.00	24.00	20.66	20.00	13.00
NiO	0.01	-	-	-	-	-	-	-	0.03	-
PbO	0.01	-	-	-	-	-	-	-	0.01	-
SiO_2	42.00	41.52	38.93	39.55	40.73	40.78	42.75	36.05	36.52	42.28
SnO_2	3.19	2.66	1.00	1.02	-	-	2.78	-	-	0.84
TiO_2	-	-	4.00	4.06	3.00	3.00	-	-	-	-
V_2O_5	-	0.91	-	-	-	-	-	0.99	1.00	2.47
ZnO	2.69	2.80	2.80	2.84	4.00	3.00	2.78	2.95	3.00	2.87
ZrO_2	6.44	6.00	5.96	6.05	6.00	6.00	6.05	2.95	3.00	3.83
Cl	0.23	0.67	0.67	0.10	0.67	0.67	0.10	1.17	0.65	0.01
F	0.09	-	-	-	-	-	-	-	0.19	0.09
P_2O_5	0.14	-	-	-	-	-	-	-	0.27	0.04
SO_3	0.41	0.80	0.70	0.10	0.70	0.70	0.30	1.10	1.20	1.25
Re_2O_7	0.10	0.10	0.10	0.10	0.10	0.10	0.10	0.10	0.10	0.10
Total	100.0	100.0	100.0	100.0	100.0	100.0	100.0	100.0	100.0	100.0

- Empty data field

Table 2.3. Elemental Compositions and Properties of the Twenty IDF Glasses.

Glass ID / Atom %	IDF1-B2	IDF2-G9	IDF3-F7	IDF4-A15	IDF5-A20	IDF6-D6	IDF7-E12	IDF8-A125	IDF9-A187	IDF10-Zr6	IDF11-G27	IDF12-A38	IDF13-A51	IDF14-A59	IDF15-A57	IDF16-A58	IDF17-A60	IDF18-A161	IDF19-C100	IDF20-F6
Al	9.34	6.45	7.84	8.87	6.25	9.37	6.95	5.31	9.57	4.72	5.81	6.56	9.49	9.65	9.97	9.87	6.36	9.13	9.28	7.83
B	9.99	11.89	12.66	11.82	12.04	13.39	13.18	13.17	16.94	16.45	11.18	11.37	10.98	11.17	11.04	11.87	12.24	17.99	18.30	12.66
Ca	0.93	2.34	8.05	2.83	2.84	6.66	8.35	1.66	5.33	2.11	2.36	2.68	0.85	0.87	1.28	0.00	2.89	6.53	6.66	8.05
Fe	0.66	0.12	0.13	0.55	0.11	0.17	0.14	3.24	0.52	4.08	0.17	0.16	0.11	0.11	0.03	0.15	0.11	0.57	0.58	0.17
K	0.12	5.95	0.49	0.55	0.54	0.17	0.55	4.29	0.50	0.56	6.00	0.54	0.54	0.54	0.54	0.53	0.54	0.43	0.15	0.54
Li	0.00	0.00	13.52	0.00	0.00	0.00	7.79	0.00	0.00	0.00	0.00	0.00	0.00	0.00	0.00	0.00	0.00	0.00	0.00	10.88
Mg	1.30	1.16	1.12	1.09	1.09	1.17	1.21	1.72	1.03	1.75	0.54	1.17	2.28	2.32	0.00	1.82	1.11	1.14	1.16	1.13
Na	38.42	32.95	17.90	37.05	37.13	33.60	24.12	30.99	34.27	33.38	33.30	37.32	36.90	36.96	36.98	36.58	37.20	30.90	30.05	19.76
Si	31.61	33.03	32.60	31.18	33.70	29.25	32.02	34.21	26.67	31.48	34.34	33.30	30.87	31.41	32.36	32.05	34.17	27.81	28.30	33.14
Sn	0.34	0.92	0.00	0.87	0.87	0.00	0.00	0.00	0.31	0.00	1.04	0.85	0.32	0.32	0.00	0.00	0.89	0.00	0.00	0.26
Ti	0.00	0.00	0.00	0.00	0.00	0.00	0.00	1.17	0.00	0.00	0.00	0.00	2.39	2.43	1.80	1.78	0.00	0.00	0.00	0.00
V	1.05	0.00	1.27	0.00	0.00	1.02	0.89	0.00	0.49	0.00	0.00	0.48	0.00	0.00	0.00	0.00	0.00	0.50	0.51	1.28
Zn	2.14	2.03	1.66	1.43	1.61	1.72	1.84	1.70	1.70	0.90	1.62	1.66	1.64	1.67	2.35	1.74	1.64	1.68	1.72	1.66
Zr	2.10	2.24	1.47	2.29	2.32	1.53	1.34	1.13	1.12	3.75	2.57	2.35	2.30	2.34	2.32	2.30	2.36	1.11	1.13	1.46
Cl	0.15	0.32	0.01	0.92	0.91	0.47	0.03	0.30	0.83	0.27	0.32	0.91	0.90	0.13	0.90	0.89	0.14	1.53	0.85	0.01
F	1.23	0.23	0.19	0.00	0.00	0.45	0.49	0.81	0.00	0.20	0.23	0.00	0.00	0.00	0.00	0.00	0.00	0.00	0.47	0.22
S	0.31	0.12	0.87	0.36	0.42	0.71	0.88	0.22	0.55	0.25	0.25	0.48	0.42	0.06	0.42	0.41	0.18	0.64	0.70	0.74
Others*	0.32	0.27	0.20	0.19	0.17	0.32	0.24	0.08	0.17	0.10	0.27	0.17	0.02	0.02	0.02	0.02	0.17	0.04	0.15	0.20
Sum**	100.0	100.0	100.0	100.0	100.0	100.0	100.0	100.0	100.0	100.0	100.0	100.0	100.0	100.0	100.0	100.0	100.0	100.0	100.0	100.0
Properties																				
PCT-A (B) (g/m^2)	0.84	0.74	0.17	0.66	0.72	0.56	0.25	0.96	1.71	0.70	0.66	0.73	0.37	–	0.21	0.31	–	0.67	0.52	0.16
PCT-A (Na) (g/m^2)	0.77	0.77	0.36	0.68	0.73	0.67	0.40	0.81	1.46	0.55	0.77	0.68	0.54	–	0.50	0.49	–	0.67	0.43	0.34
VHT 24-day rate ($g/m^2/d$)	110	41 to 50[$]	18	25	7	5 to 18[$]	31 to 41[$]	38	25 to 73[$]	0.6	13 to 57[$]	8 to 32[$]	2 to 32[$]	22	63 to 75[$]	25 to 33[$]	5	25 to 68[$]	10 to 14[$]	13 to 17[$]
Viscosity (P) 1100°C	131	86	32	112	95	48	34	104	33	58	102	98	119	–	150	150	–	44	52	40
Conductivity (S/m) 1100°C	0.644	0.464	0.349	0.598	0.444	0.392	0.457	0.327	0.47	0.433	0.451	0.552	0.568	–	0.504	0.477	–	0.311	0.240	–
K3 Neck Loss (inch)	0.039	0.038	0.01	0.036	0.033	0.0395	0.031	0.0255	0.0325	–	0.034	0.043	0.0315	–	0.027	0.022	–	0.0325	0.036	0.012

*Cs, Cr, Ni, Pb, P, Re ; ** Atom % excludes oxygen; - Empty data field; [$] Duplicate test results

Table 3.1. Summary of Long-term PCT on the Twenty IDF Glasses.

Glass ID	IDF1-B2	IDF2-G9	IDF3-F7	IDF4-A15	IDF5-A20	IDF6-D6	IDF7-E12	IDF8-A125	IDF9-A187	IDF10-Zr6	IDF11-G27	IDF12-A38	IDF13-A51	IDF14-A59	IDF15-A57	IDF16-A58	IDF17-A60	IDF18-A161	IDF19-C100	IDF20-F6
Tests at 120°C and S/V 20,000 m^{-1}																				
Immersion date	09/21/2010	09/21/2010	06/24/2010	09/21/2010	09/21/2010	09/22/2010	09/22/2010	09/22/2010	09/22/2010	09/22/2010	Not tested									
Duration (d)	119	119	56	119	119	56	56	119	56	119										
Resumption (d)	Nearing	NO	56	NO	NO	56	56	Slow rise	56	NO										
Status	Terminated after 272 days																			
Tests at 90°C and S/V 20,000 m^{-1}																				
Immersion date	06/24/2010	06/24/2010	06/24/2010	07/15/2010	07/15/2010	07/15/2010	06/24/2010	06/24/2010	07/15 2010	07/15/2010	06/09/2015	06/09/2015	06/09/2015	06/09/2015	06/09/2015	06/10/2015	06/10/2015	06/10/2015	06/10/2015	06/10/2015
Duration (d)	272	272	272	272	272	180	181	272	180	272	730	730	730	730	730	730	730	730	730	730
Resumption(d)	Nearing	NO	NO	Nearing	NO	56	120	Plateau	56	NO	NO	NO	Nearing	273	Nearing	NO	NO	119	119	365
Status	Terminated after 272 days										Ongoing									
Tests at 90°C and S/V 2,000 m^{-1}																				
Immersion date	06/16/2010	06/16/2010	06/16/2010	07/13/2010	07/13/2010	07/13/2010	06/16/2010	06/16/2010	07/13/2010	07/13/2010	Not tested									
Duration (d)	2546	2546	2546	2526	2526	1877	2546	2546	1877	2526										
Resumption (d)	NO	NO	2177	1805	Nearing	545	1266	909	365	NO										
Status*	O	O	O	O	O	T	O	O	T	O										
Tests at 40°C and S/V 2,000 m^{-1}																				
Immersion date	06/22/2010	06/22/2010	06/22/2010	07/14/2010	07/14/2010	07/14/2010	06/22/2010	06/22/2010	07/14/2010	07/14/2010	Not tested									
Duration (d)	2541	2541	2541	2526	2526	2526	2541	2541	2526	2526										
Status	Ongoing tests – No resumption – steady at 1% alteration							O/steady at 3%	O/steady at 1%											

* O=Ongoing, T=Terminated

Table 3.2. Long-Term PCT-B Results at 90°C and S/V 20,000 m^{-1}.

Glass ID	Test	Immersion Date	Sampling Date	Period	pH	B* Norm. Release [g/L]	K* Norm. Release [g/L]	Li* Norm. Release [g/L]	Na* Norm. Release [g/L]	Si* Norm. Release [g/L]
IDF11-G27CCC	ILHC	6/9/2015	6/16/2015	7	12.31	5.41	4.47	-	7.35	0.91
			7/7/2015	28	12.61	8.25	6.16	-	10.64	1.42
			8/4/2015	56	12.65	9.54	6.84	-	11.09	1.64
			10/6/2015	119	12.71	10.06	7.79	-	12.59	1.66
			12/8/2015	182	12.83	12.41	9.31	-	16.42	2.08
			3/8/2016	273	12.91	13.68	10.19	-	17.03	2.42
			6/7/2016	364	12.93	15.64	10.34	-	23.62	3.00
			12/8/2016	548	13.26	35.67	20.10	-	32.92	10.07
			6/8/2017	730	13.28	41.71	18.98	-	37.71	11.30
IDF12-A38CCC	ILHC	6/9/2015	6/16/2015	7	12.16	4.59	3.02	-	5.47	0.90
			7/7/2015	28	12.41	6.85	4.08	-	8.82	1.33
			8/4/2015	56	12.47	7.94	4.97	-	9.11	1.51
			10/6/2015	119	12.53	8.08	4.95	-	9.94	1.48
			12/8/2015	182	12.66	13.96	9.75	-	14.16	2.70
			3/8/2016	273	12.71	20.64	13.01	-	21.47	4.11
			6/7/2016	364	12.75	29.94	12.93	-	26.47	5.02
			12/8/2016	548	12.87	41.59	20.77	-	34.99	6.50
			6/8/2017	730	12.94	58.12	32.69	-	37.55	9.53
IDF13-A51CCC	ILHC	6/9/2015	6/16/2015	7	12.05	3.08	2.06	-	4.07	0.61
			7/7/2015	28	12.33	5.61	2.79	-	6.31	0.92
			8/4/2015	56	12.43	6.61	3.55	-	6.87	1.01
			10/6/2015	119	12.50	8.51	3.51	-	8.27	1.08
			12/8/2015	182	12.64	9.97	4.51	-	9.70	1.20
			3/8/2016	273	12.70	11.54	5.08	-	11.94	1.29
			6/7/2016	364	12.73	16.88	7.08	-	19.65	1.79
			12/8/2016	548	12.86	104.36	38.01	-	62.76	5.70
			6/8/2017	730	13.33	197.31	71.53	-	79.53	8.10
IDF14-A59CCC	ILHC	6/9/2015	6/16/2015	7	12.11	2.64	2.09	-	4.25	0.64
			7/7/2015	28	12.37	5.03	2.54	-	7.13	1.05
			8/4/2015	56	12.48	6.39	3.77	-	7.43	1.25
			10/6/2015	119	12.54	9.53	4.88	-	10.38	1.33
			12/8/2015	182	12.77	22.09	9.65	-	17.67	2.37
			3/8/2016	273	12.81	132.61	52.46	-	65.30	6.45
			6/7/2016	364	12.85	268.65	97.56	-	188.44	10.54
			12/8/2016[$]	548[$]	13.16	740.66	289.77	-	289.54	25.93
			6/8/2017	730	13.66	1,003.04	426.20	-	413.12	40.60
IDF15-A57CCC	ILHC	6/9/2015	6/16/2015	7	12.04	2.05	1.74	-	3.85	0.60
			7/7/2015	28	12.33	3.63	2.31	-	5.86	0.97
			8/4/2015	56	12.45	4.71	2.80	-	6.45	1.14
			10/6/2015	119	12.51	6.29	3.10	-	7.80	1.04
			12/8/2015	182	12.74	9.28	4.00	-	9.15	1.36
			3/8/2016	273	12.81	23.67	8.15	-	16.29	2.42
			6/7/2016	364	12.86	58.46	16.48	-	46.18	5.07
			12/8/2016	548	13.16	140.46	48.64	-	76.18	11.07
			6/8/2017	730	13.68	244.16	85.55	-	132.40	25.82

- Below detection limit; *Normalized release calculated from average of triplicate tests with less than 10%RSD (median 0.6% RSD)

[$]Altered glass removed from one of the triplicate vessels

Table 3.2. Long-Term PCT-B Results at 90°C and S/V 20,000 m^{-1} (continued).

Glass ID	Test	Immersion Date	Sampling Date	Period	pH	B* Norm. Release [g/L]	K* Norm. Release [g/L]	Li* Norm. Release [g/L]	Na* Norm. Release [g/L]	Si* Norm. Release [g/L]
IDF16-A58CCC	ILHD	6/10/2015	6/17/2015	7	12.17	3.76	1.55	-	4.00	0.58
			7/8/2015	28	12.32	7.64	2.84	-	6.57	0.79
			8/5/2015	56	12.44	8.75	3.11	-	7.24	0.93
			10/7/2015	119	12.51	10.46	3.39	-	8.29	1.05
			12/9/2015	182	12.65	12.71	4.02	-	9.89	1.24
			3/9/2016	273	12.71	16.38	5.11	-	12.12	1.70
			6/9/2016	365	12.74	18.68	5.46	-	14.16	2.00
			12/8/2016	547	12.84	23.69	8.21	-	15.47	2.27
			6/9/2017	730	12.93	41.06	11.85	-	21.68	3.49
IDF17-A60CCC	ILHD	6/10/2015	6/17/2015	7	12.26	4.30	2.46	-	5.43	0.95
			7/8/2015	28	12.42	6.77	4.07	-	8.46	1.42
			8/5/2015	56	12.48	7.31	4.37	-	8.91	1.58
			10/7/2015	119	12.54	7.69	4.67	-	9.94	1.74
			12/9/2015	182	12.74	11.07	5.86	-	12.58	2.48
			3/9/2016	273	12.81	16.15	9.66	-	15.44	3.64
			6/9/2016	365	12.84	24.79	12.59	-	24.65	5.19
			12/8/2016	547	12.94	38.48	21.01	-	27.50	6.62
			6/9/2017	730	12.98	46.84	23.63	-	32.46	8.38
IDF18-A161CCC	ILHD	6/10/2015	6/17/2015	7	11.53	7.30	3.17	-	6.28	0.50
			7/8/2015	28	11.87	8.77	4.48	-	7.66	0.65
			8/5/2015	56	11.98	9.23	4.76	-	8.16	0.87
			10/7/2015	119	12.22	14.84	7.82	-	12.17	1.24
			12/9/2015	182	12.33	210.83	112.87	-	139.43	1.40
			3/9/2016	273	12.41	394.29	196.67	-	225.99	1.87
			6/9/2016	365	12.43	544.32	227.03	-	340.78	1.93
			12/8/2016[$]	547[$]	12.77	684.90	343.36	-	376.92	2.64
			6/9/2017	730	12.88	564.15	288.33	-	401.11	2.89
IDF19-C100CCC	ILHD	6/10/2015	6/17/2015	7	11.58	5.81	4.17	-	4.88	0.43
			7/8/2015	28	11.92	7.85	5.09	-	6.85	0.61
			8/5/2015	56	12.03	8.69	5.75	-	7.22	0.80
			10/7/2015	119	12.32	10.67	6.02	-	8.94	0.96
			12/9/2015	182	12.43	71.58	47.17	-	49.32	1.39
			3/9/2016	273	12.52	419.94	328.34	-	241.22	2.27
			6/9/2016	365	12.55	420.48	272.00	-	284.94	2.13
			12/8/2016[$]	547[$]	11.86	485.63	318.15	-	331.13	2.60
			6/9/2017	730	11.93	454.48	307.74	-	348.67	2.92
IDF20-F6CCC	ILHD	6/10/2015	6/17/2015	7	11.54	1.60	1.37	2.35	2.26	0.47
			7/8/2015	28	11.85	1.94	1.53	3.08	3.22	0.65
			8/5/2015	56	11.94	2.04	1.67	3.35	3.52	0.74
			10/7/2015	119	12.15	2.44	1.66	3.99	4.51	0.82
			12/9/2015	182	12.26	3.74	2.38	5.57	5.73	1.04
			3/9/2016	273	12.32	11.35	6.59	10.99	11.08	1.59
			6/9/2016	365	12.35	337.31	107.88	196.55	233.60	2.63
			12/8/2016[$]	547[$]	11.66	459.43	192.73	232.94	299.54	3.37
			6/9/2017	730	11.86	641.69	212.38	276.99	378.30	4.95

- Below detection limit; *Normalized release calculated from average of triplicate tests with less than 10%RSD (median 0.6%RSD); [$]Altered glass removed from one of the triplicate vessels

Table 3.2. Long-Term PCT-B Results at 90°C and S/V 20,000 m^{-1}(continued).

Glass ID	Test	Immersion Date	Sampling Date	Period	pH	B* Norm. Release [g/L]	K* Norm. Release [g/L]	Li* Norm. Release [g/L]	Na* Norm. Release [g/L]	Si* Norm. Release [g/L]
ANL-LRM-2	ILHC	6/9/2015	6/16/2015	7	12.02	6.60	2.07	-	5.83	0.88
			7/7/2015	28	12.31	13.34	3.35	-	11.13	1.28
			8/4/2015	56	12.42	17.06	3.93	-	11.72	1.36
			10/6/2015	119	12.47	22.76	4.79	3.12	18.44	2.50
			12/8/2015	182	12.57	41.77	10.40	7.30	27.94	8.61
			3/8/2016	273	12.61	143.10	28.47	74.81	96.66	27.56
			6/7/2016	364	12.66	699.96	125.34	404.69	496.12	9.61
			12/8/2016[$]	548	12.43	918.89	169.37	599.61	710.94	205.39
			6/8/2017	730	12.47	729.60	157.64	605.12	527.29	18.20
ANL-LRM-2	ILHD	6/10/2015	6/17/2015	7	12.03	6.80	1.90	-	5.88	0.91
			7/8/2015	28	12.31	13.22	3.40	-	11.00	1.28
			8/5/2015	56	12.43	17.22	3.99	-	12.02	1.37
			10/7/2015	119	12.47	23.12	5.11	2.54	18.55	2.12
			12/9/2015	182	12.54	47.98	10.61	11.30	30.81	9.73
			3/9/2016	273	12.61	119.70	22.95	61.66	75.74	22.92
			6/9/2016	365	12.66	581.49	106.92	354.90	453.58	8.17
			12/8/2016[$]	547	12.45	1000.19	191.78	594.14	767.94	177.58
			6/9/2017	730	12.48	789.10	173.24	589.47	580.22	46.24

- Below detection limit; *Normalized release calculated from average of triplicate tests with less than 10%RSD (median 0.6%RSD)); [$]Altered glass removed from one of the triplicate vessels

Table 4.1. Summary of Phases Identified on Solid Samples Taken from PCT Vessels of the Ten IDF Phase 1 Glasses [45].

Sample ID	Resumption?	Phyllosilicates	Tecto- and Soro-silicates	Others
Sampled from PCT-B at 90°C and S/V 20,000 m^{-1}				
IDF1-B2CCC	272 days	Saponite	Lazurite	-
IDF2-G9CCC	No	None detectable		
IDF3-F7CCC	No	None detectable		$^{\$}ZnCr_2O_4$
IDF4-A15CCC in BHHF4-3	272 days	None detectable	Phillipsite and Lazurite	-
IDF5-A20CCC	No	None detectable	Gehlenite	-
IDF6-D6CCC in BHHF6	56 to 120 days	Agglomeration– sampling not possible		
IDF7-E12CCC in ILHA-15	180 days	Agglomeration– sampling not possible		
IDF8-A125CCC in AHHF8-15	No	None detectable	Analcime	-
IDF9-A187CCC in BHHF9	56 to 120 days	Agglomeration – sampling not possible		
IDF10-Zr6CCC	No	None detectable		
Sampled from PCT-B at 90°C and S/V 2,000 m^{-1}				
IDF1-B2CCC	Possibly on-going	No sampling		
IDF2-G9CCC in ALHF3-9	No	No sampling		
IDF3-F7CCC in ALHF3-9	2546 days	None detectable		$^{\$}ZnCr_2O_4$
IDF4-A15CCC in BLHF4-3	1445 days and on-going	None detectable	Phillipsite and Lazurite	-
IDF5-A20CCC	2546 days and on-going	No sampling		
IDF6-D6CCC in BLHF6-(9+10)-15	545 to 727 days	Lizardite	Analcime and Gobbinsite	-
IDF7-E12CCC in ILHA-15	1266 days	Tobermorite and Kaolinite	Phillipsite and Coesite	-
IDF8-A125CCC in ALHF8-15	727 to 1630 days	None detectable	Analcime	-
IDF9-A187CCC in BLHF9-(12+13)	364 to 727 days	Lizardite	Analcime and gobbinsite	-
IDF10-Zr6CCC	No	No sampling		

$^{\$}$Trace amount of zincochromite ($ZnCr_2O_4$) originally identified in the CCC glass prior to leaching; - Empty data field

Table 4.2. Summary of Phases Identified on Solid Samples Taken from PCT Vessels of the Ten IDF Phase 2 Glasses.

Sample ID	Resumption?	Phyllosilicates	Tecto- and Soro-silicates
Sampled from PCT-B at 90°C and S/V 2,000 m^{-1}			
IDF11-G27CCC	No	No sampling	
IDF12-A38CCC	No	No sampling	
IDF13-A51CCC	Slow rise - ongoing	No sampling	
IDF14-A59CCC in ILHC-8 (vessel 12)	273 days	None clearly identified	Phillipsite $(K,Na)_2(Si,Al)_8O_{16}\cdot 4H_2O$ in XRD; $(Na_{6.7}K_{0.1}Mg_{0.4}Ca_{0.2}Ti_{0.8}Zn_{0.4})Al_2Si_7O_{24}$ in SEM
IDF15-A57CCC	Slow rise - ongoing	No sampling	
IDF16-A58CCC	No	No sampling	
IDF17-A60CCC	No	No sampling	
IDF18-A161CCC in ILHD-8 (vessel 9)	119 days	Aliettite $(Ca_{0.9}Mg_6(Si,Al)_8O_{22}(OH)_4\cdot 4H_2O)$ or beidellite $(Na_{0.3}Al_2(Si,Al)_4O_{10}(OH)_2\cdot 2H_2O)$ in XRD	Phillipsite $(K,Na)_2(Si,Al)_8O_{16}\cdot 4H_2O$ in XRD; Multiple morphologies, phillipsite or albite in SEM: $Na_6CaFe_{0.1}Zn_{0.3}Zr)Al_3Si_{10}O_{24}$
IDF19-C100CCC in ILHD-8 (vessel 12)	119 days	Aliettite $(Ca_{0.9}Mg_6(Si,Al)_8O_{22}(OH)_4\cdot 4H_2O)$ or beidellite $(Na_{0.3}Al_2(Si,Al)_4O_{10}(OH)_2\cdot 2H_2O)$ in XRD	Phillipsite $(K,Na)_2(Si,Al)_8O_{16}\cdot 4H_2O$ in XRD; Multiple morphologies, phillipsite or albite in SEM: $Na_6CaFe_{0.1}Zn_{0.3}Zr)Al_3Si_{10}O_{24}$
IDF20-F6CCC in ILHD-8 (vessel 15)	365 days	Swinefordite $(Ca_{0.1}(Li,Al)_3Si_4O_{10}(OH)_2\cdot 2(H_2O)$ in XRD; Possibly cavansite $Ca(VO)Si_4O_{10}(H_2O)_4$ in SEM	Phillipsite $(K,Na)_2(Si,Al)_8O_{16}\cdot 4H_2O$ smaller in XRD Possibly hemimorphite $Zn_4Si_2O_7(OH)_2\cdot H_2O$ in SEM
ANL-LRM2 in ILHC-8 and ILHD-8 (vessel 18 in each set)	272 days	None detectable	Phillipsite $(K,Na)_2(Si,Al)_8O_{16}\cdot 4H_2O$ and possibly analcime in XRD; Multiple morphologies, generally small in SEM: $(Na_{3.7}K_{0.1}Mg_{0.2}Ca_{0.6}Fe_{0.1}Zn_{0.41}Zr_{0.3})Al_{1.5}Si_{4.8}O_{16}$

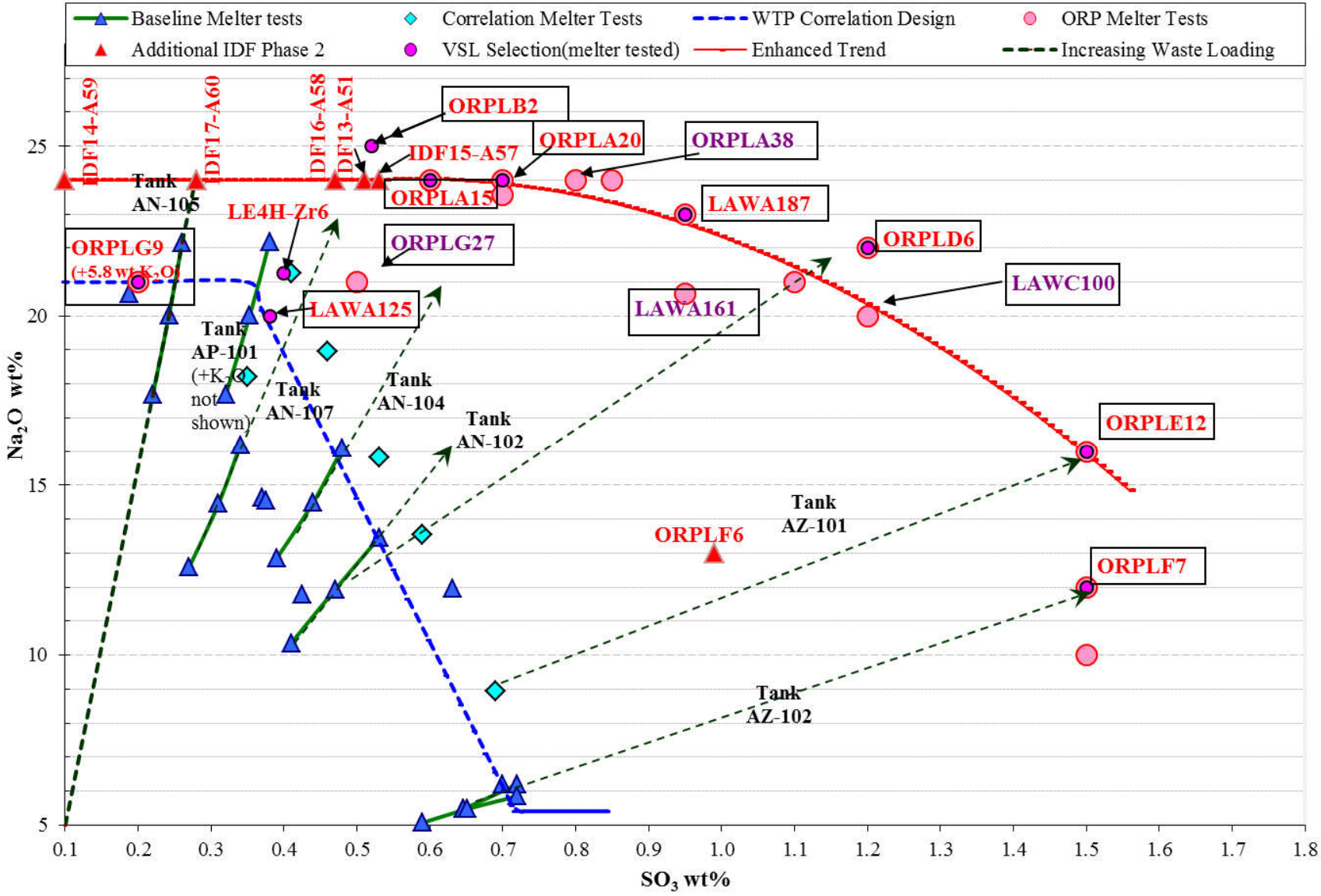

Figure 2.1. Overview of Na_2O and SO_3 loadings for WTP and ORP glasses and selected IDF glasses.

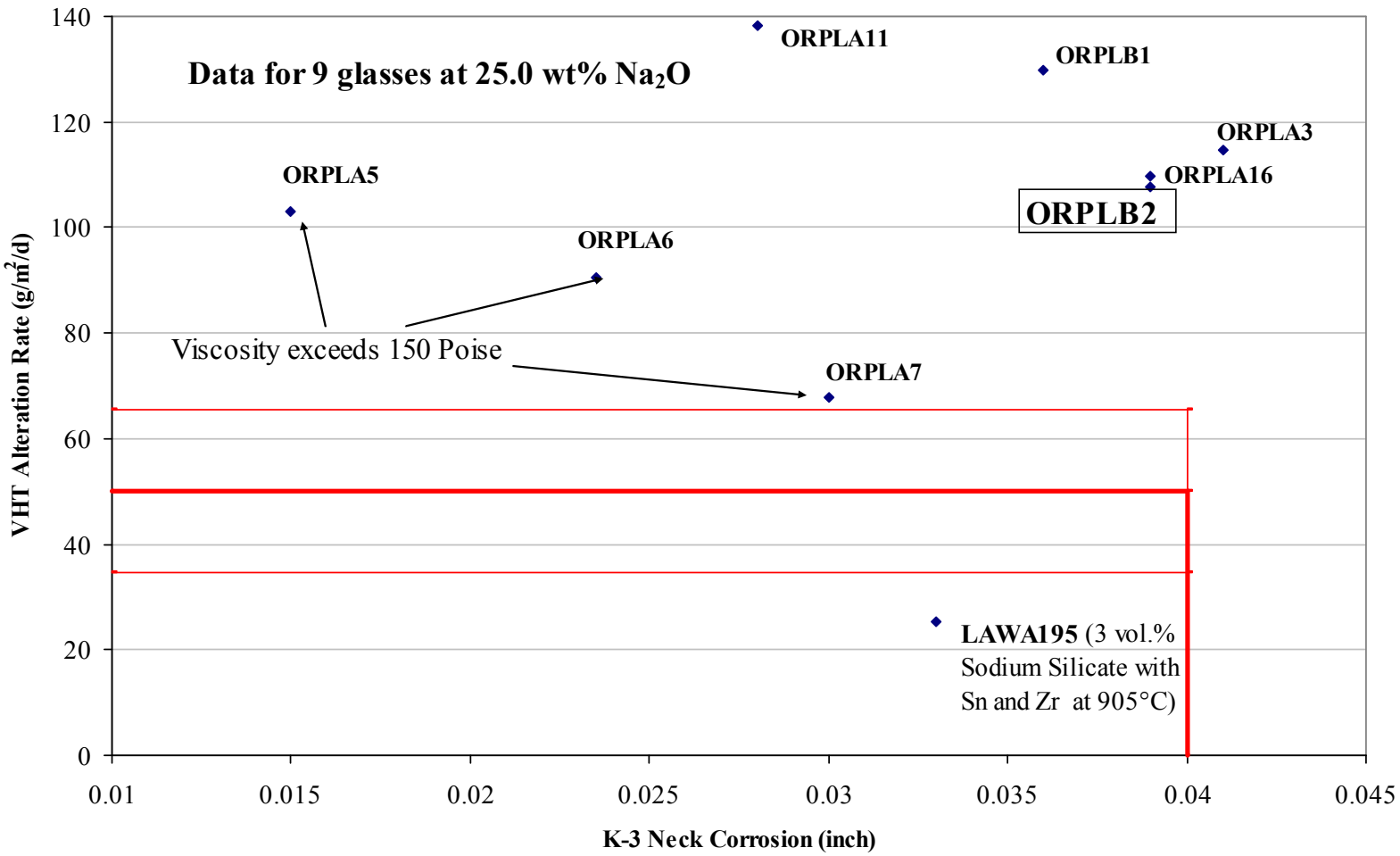

Figure 2.2. VHT alteration rate and K-3 neck corrosion for glasses with 25.0 wt% Na_2O leading to the selection of ORPLB2 as the IDF bounding glass.

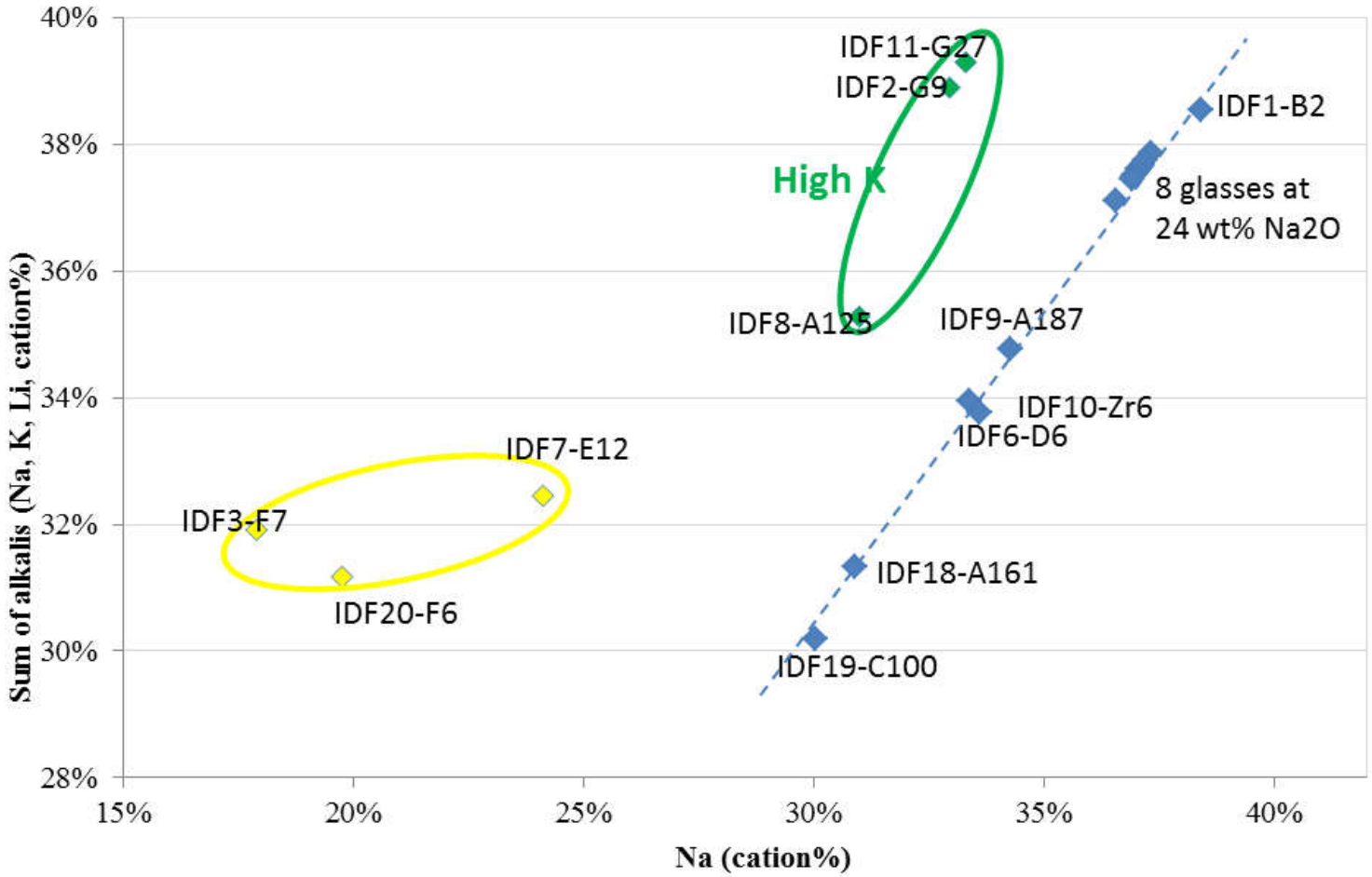

Figure 2.3. Sum of alkalis (Na, K, Li, in cation%) versus Na in the 20 IDF glasses. The three high potassium glasses are circled in green and the three high sulfate glasses containing lithium additive are circled in yellow.

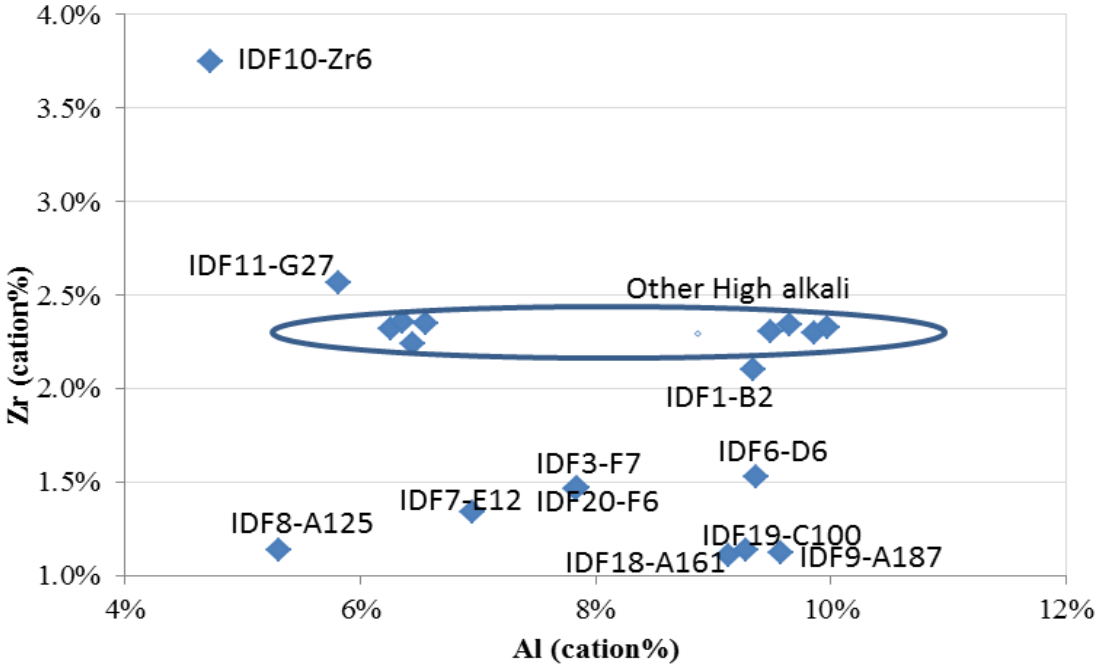

Figure 2.4. Zirconium versus aluminum in the 20 IDF glasses (cation%).

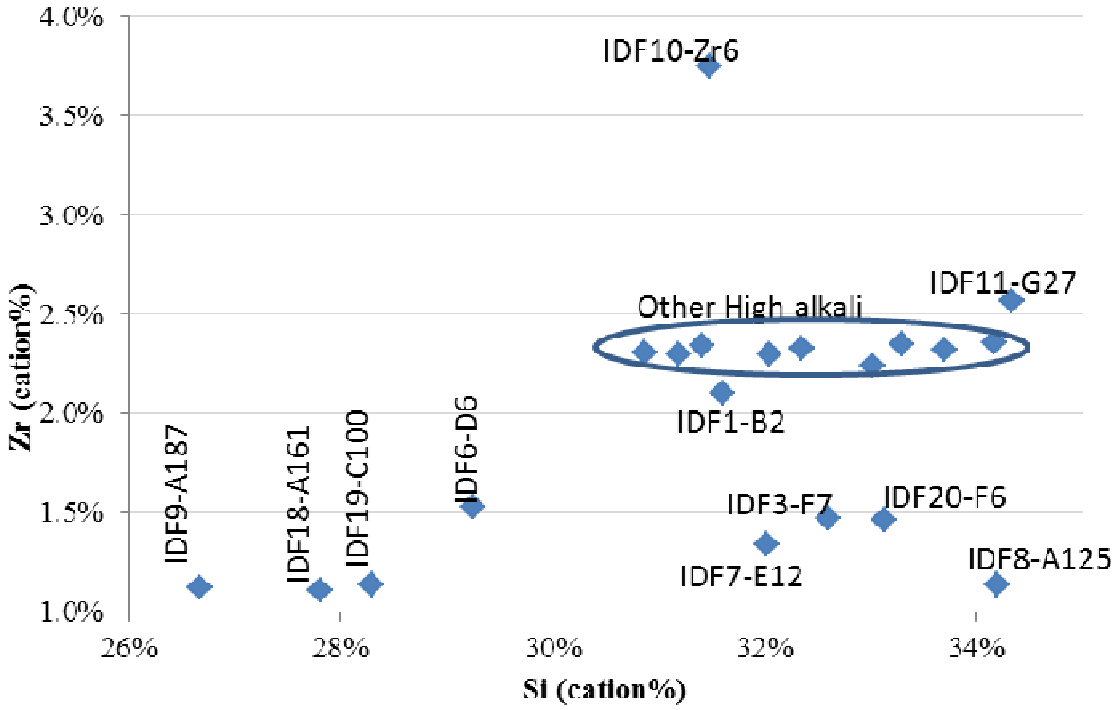

Figure 2.5. Zirconium versus silicon in the 20 IDF glasses (cation%).

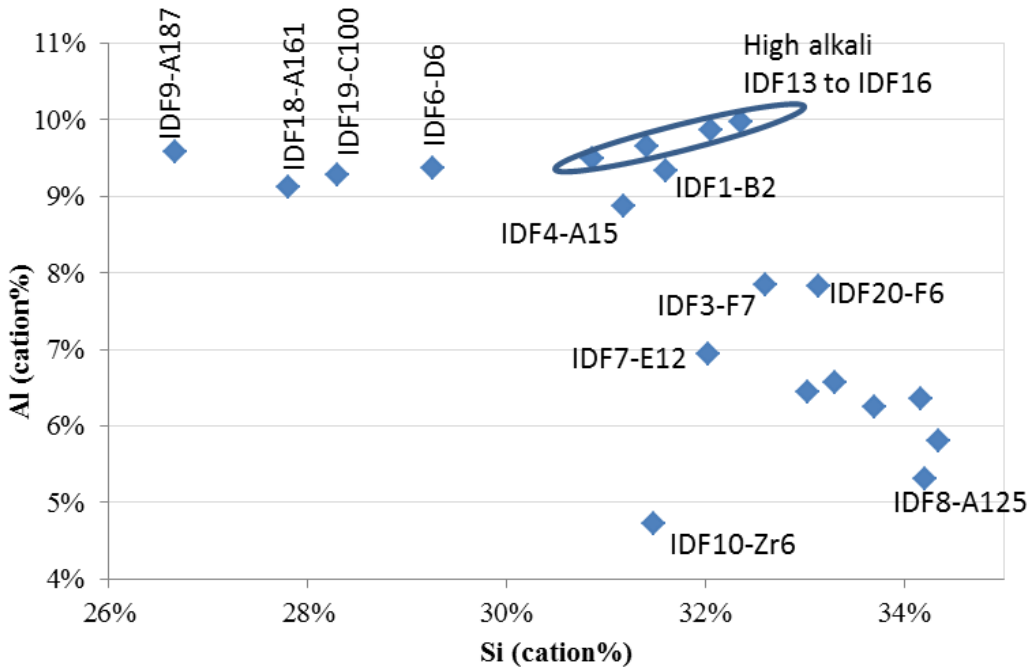

Figure 2.6. Aluminum versus silicon in the 20 IDF glasses (cation%).

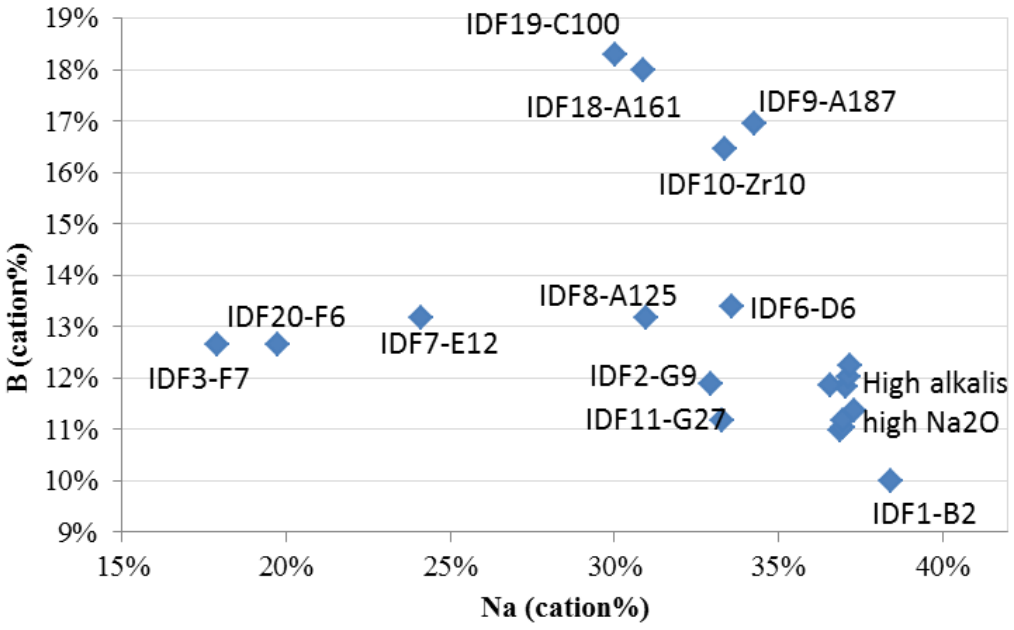

Figure 2.7. Boron versus sodium in the 20 IDF glasses (cation%).

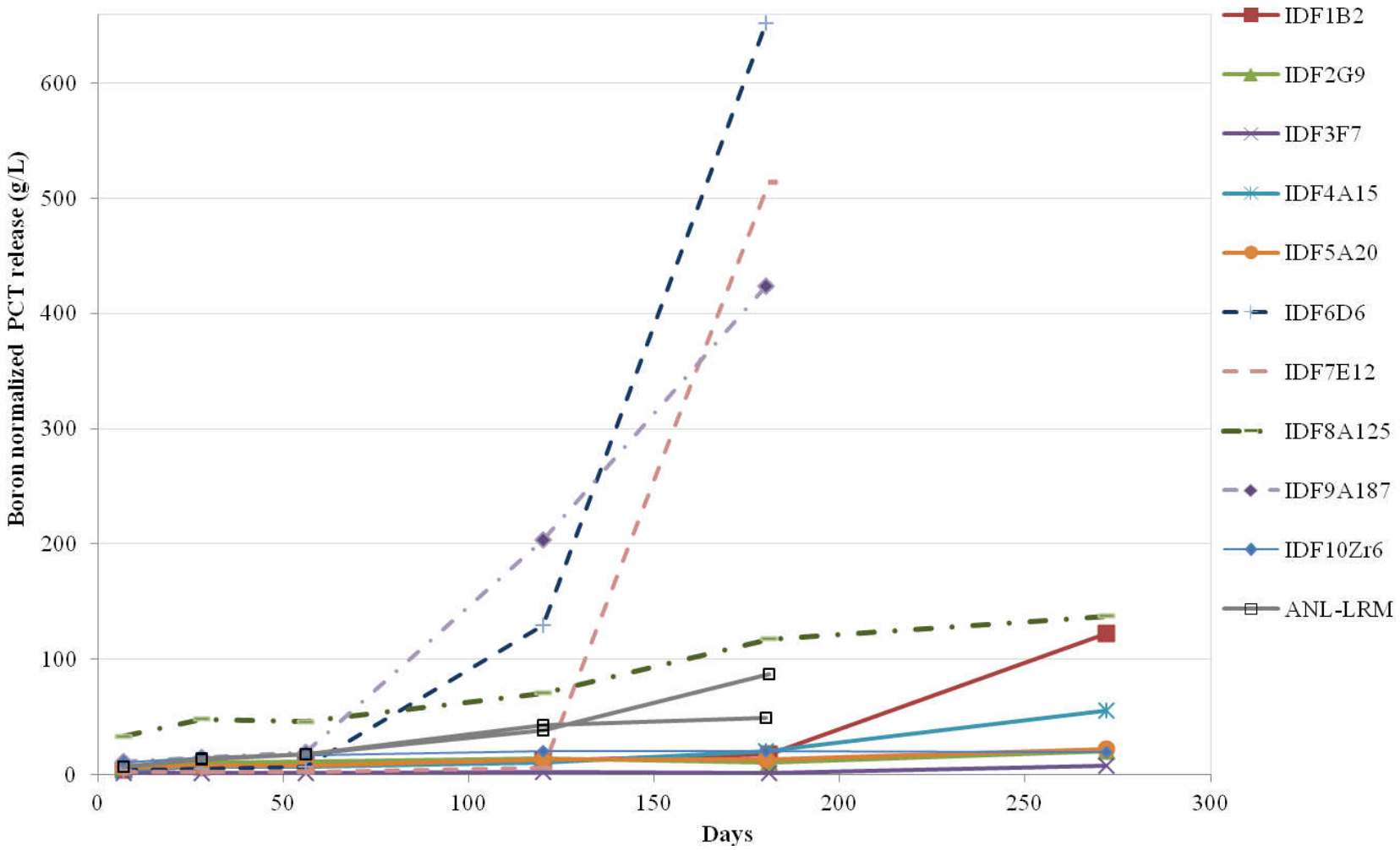

Figure 3.1. PCT-B results (90°C and S/V 20,000 m^{-1}) for the ten IDF Phase 1 glasses and the ANL-LRM2 reference glass.

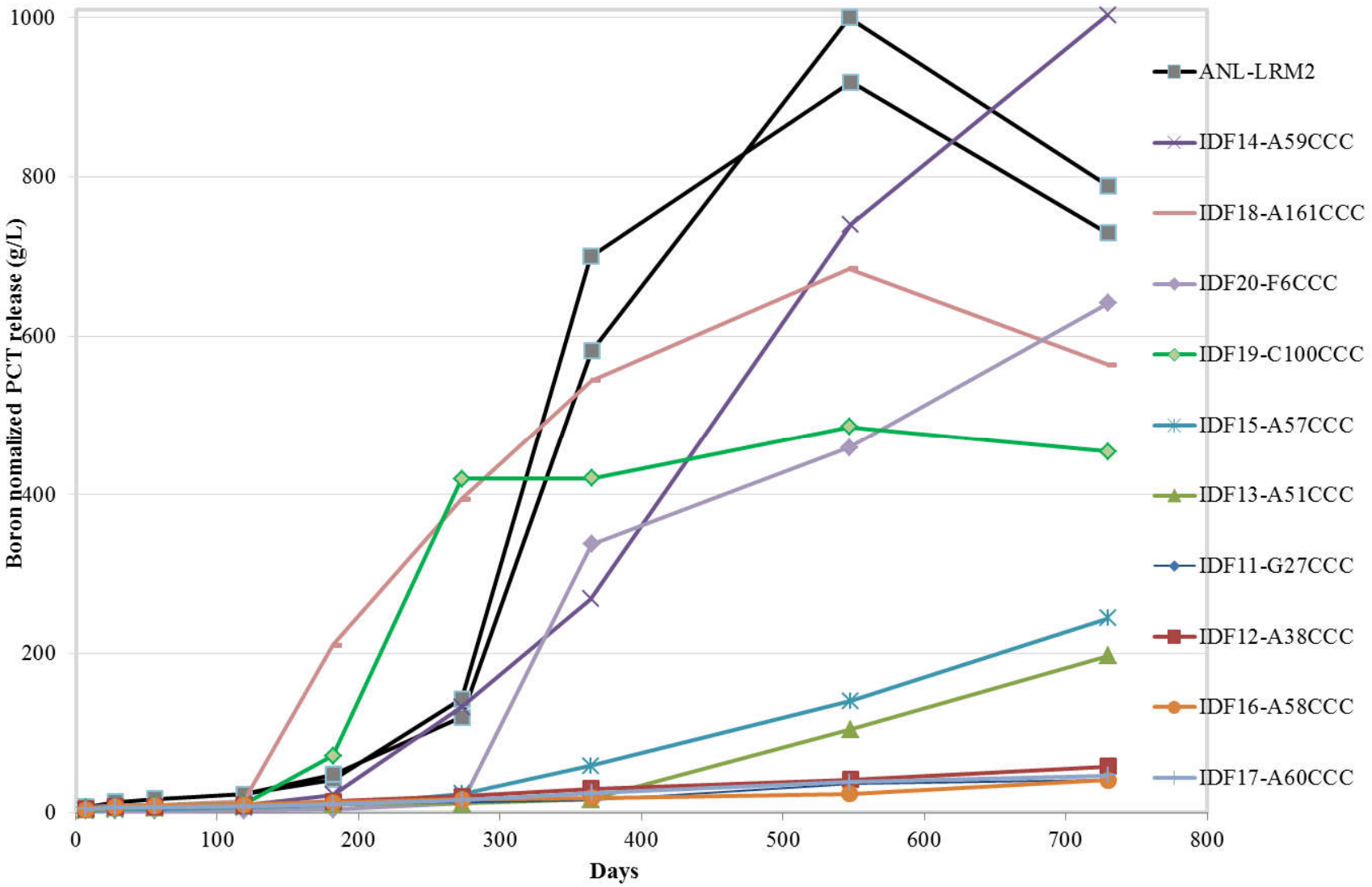

Figure 3.2. PCT-B results (90°C and S/V 20,000 m^{-1}) for the ten IDF Phase 2 glasses and the ANL-LRM2 reference glass.

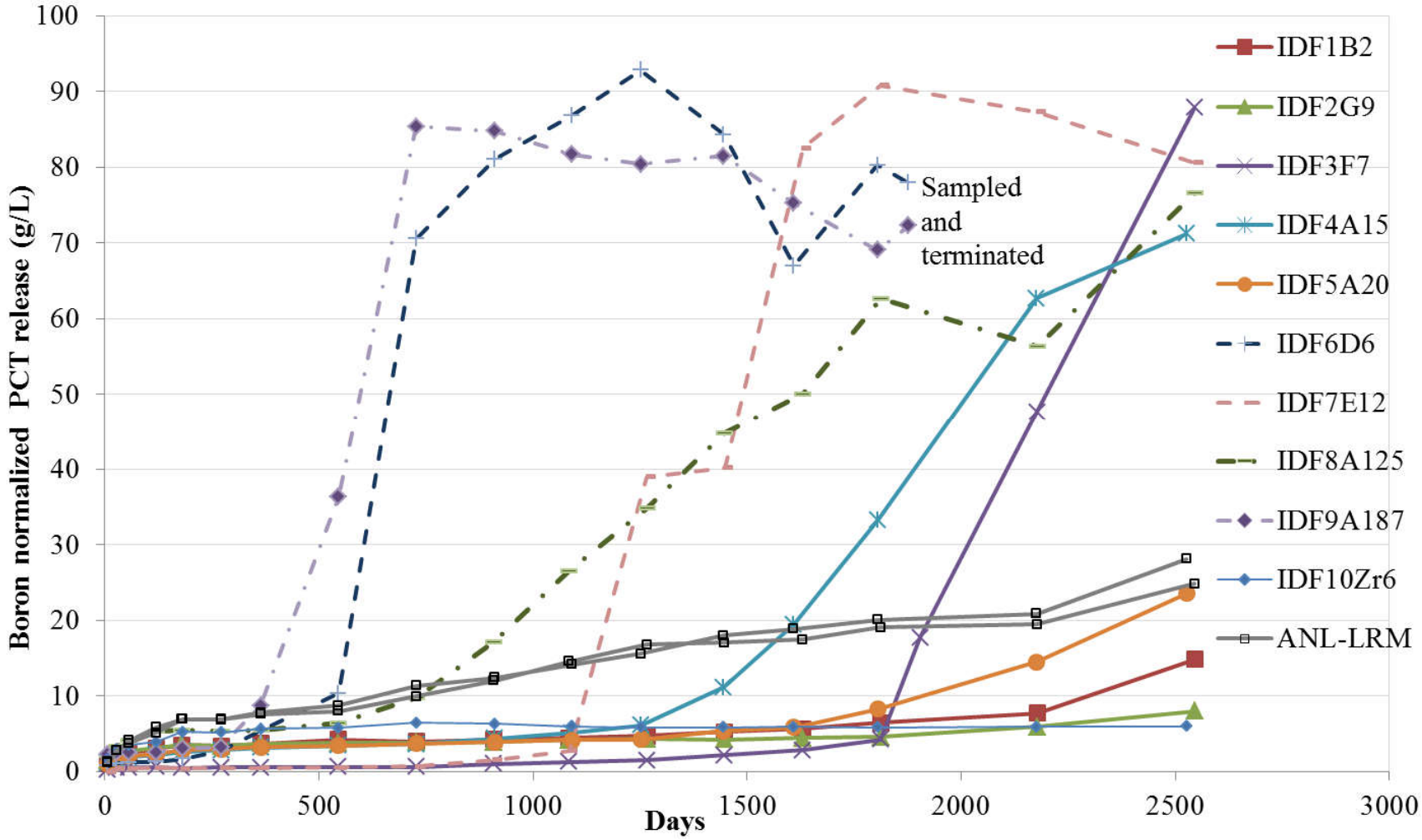

Figure 3.3. PCT-B results (90°C and S/V 2,000 m^{-1}) for the ten IDF Phase 1 glasses.

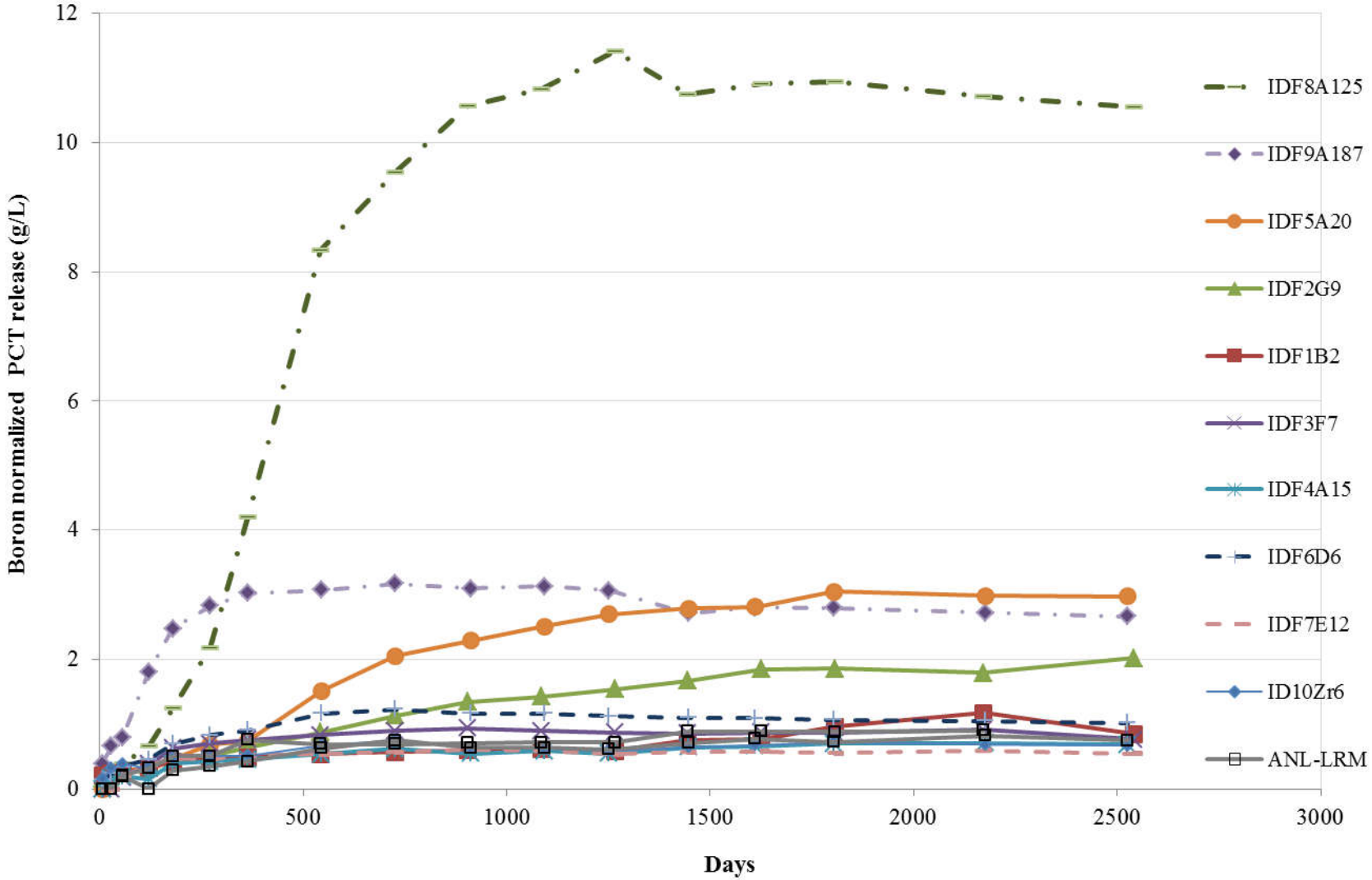

Figure 3.4. PCT-B results (40°C and S/V 2,000 m^{-1}) for the ten IDF Phase 1 glasses.

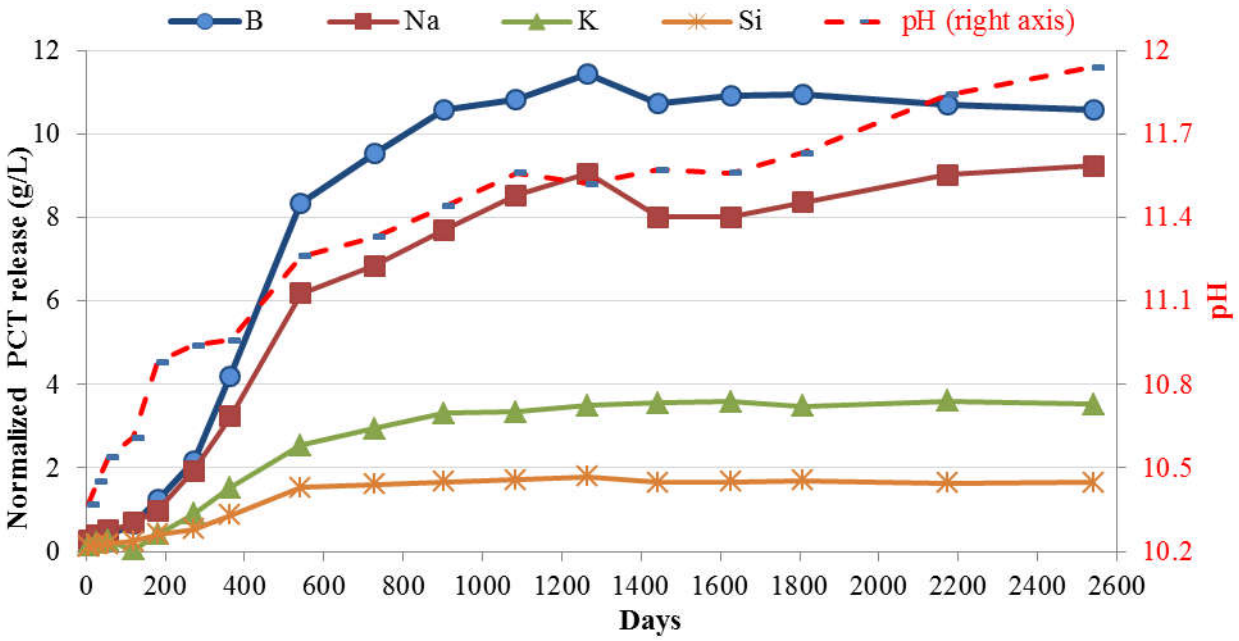

Figure 3.5. PCT-B results (40°C and S/V 2,000 m^{-1}) for IDF8-A125CCC.

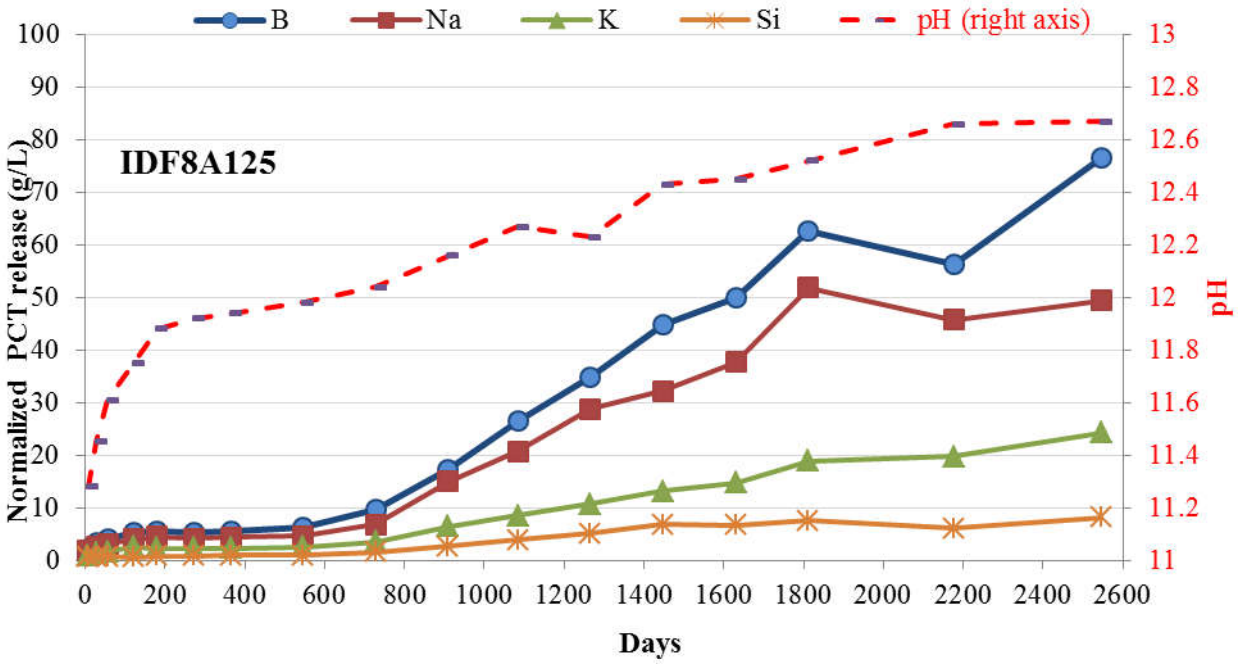

Figure 3.6. PCT-B results (90°C and S/V 2,000 m^{-1}) for IDF8-A125CCC.

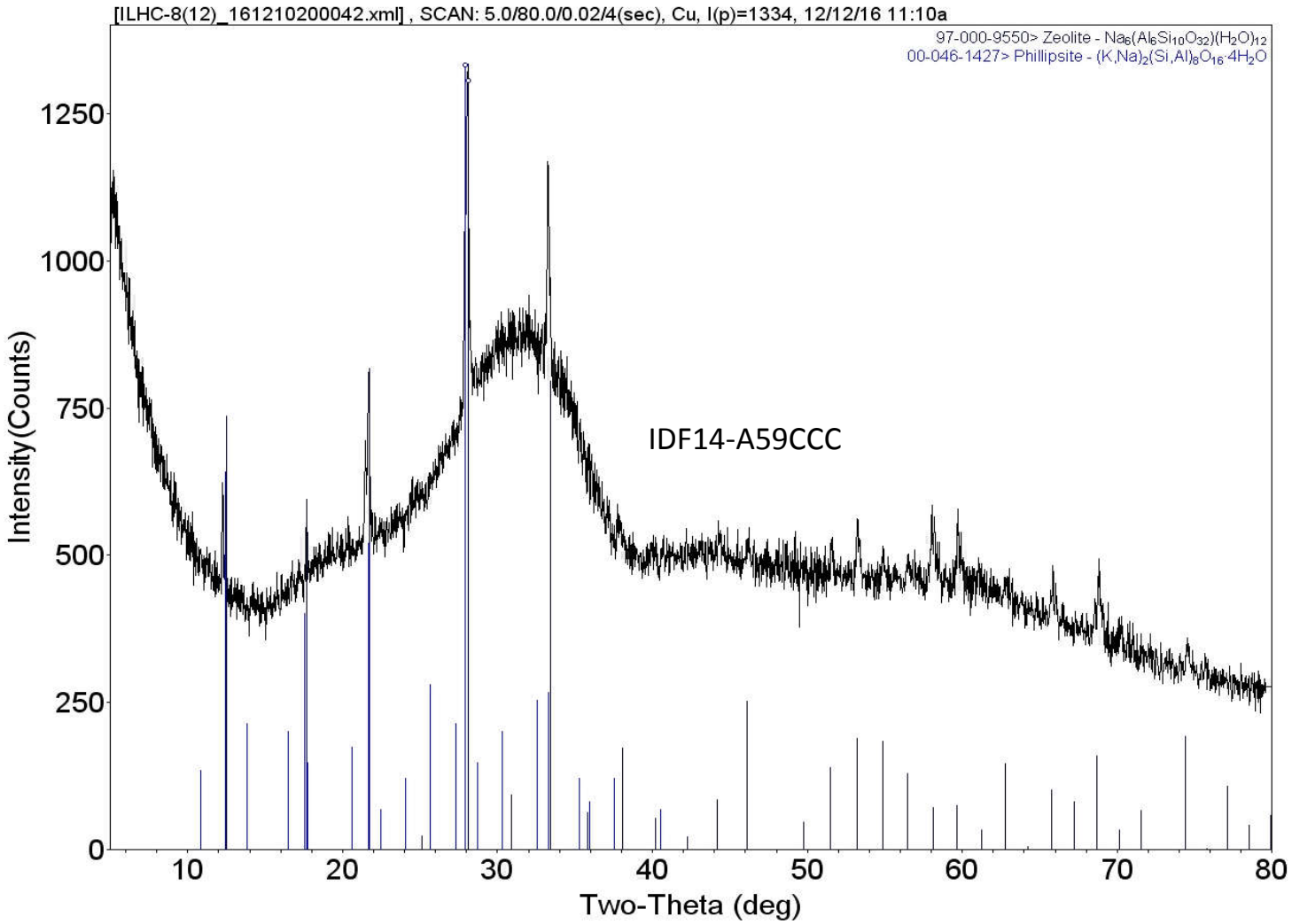

Figure 4.1. XRD powder patterns (raw data and best match) for altered IDF Phase 2 glass IDF14-A59CCC subjected to PCT for 548 days at 90°C and S/V 20,000 m^{-1}.

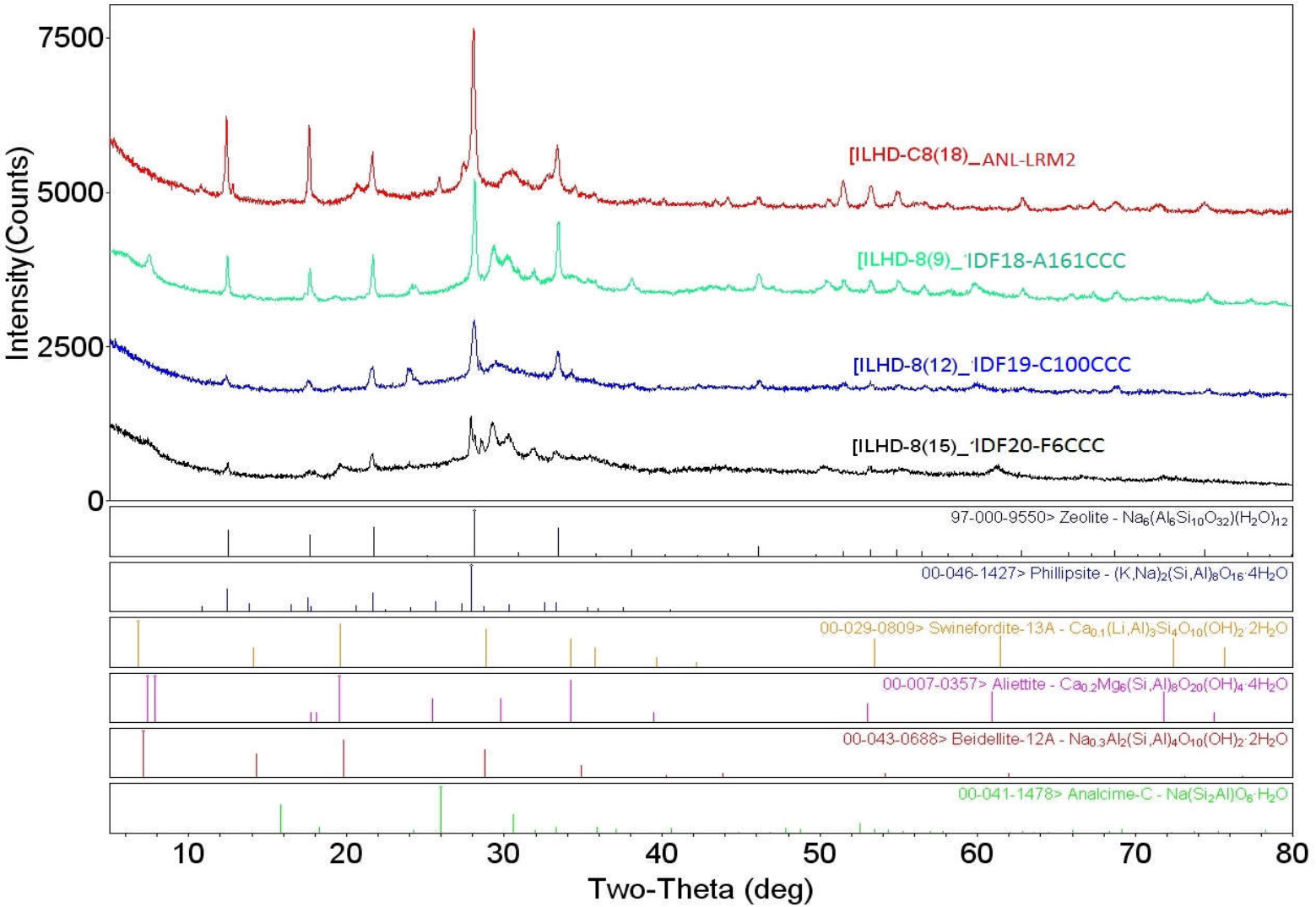

Figure 4.2. XRD powder patterns (raw data and best match) for four IDF Phase 2 glasses subjected to PCT for 547 days at 90°C and S/V 20,000 m^{-1}.

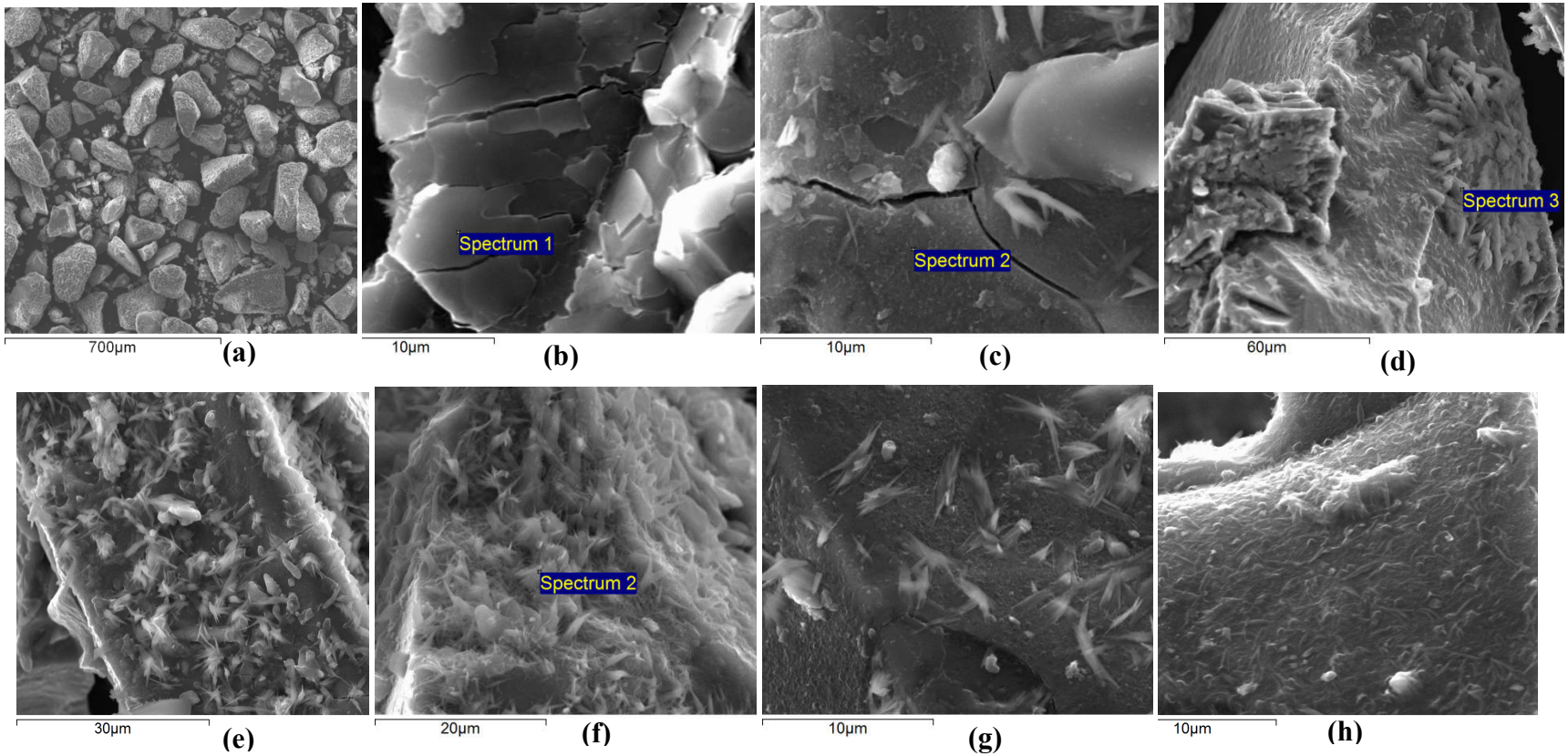

Figure 4.3. SEM micrographs of the surface of glass powder IDF14-A59CCC after 548 days of PCT-B at 90°C and 20,000 m^{-1} S/V; (a) the ~100 µm glass grains are covered with an alteration layer often fractured or spalled (as seen in b and c). One type of crystal dominates: a euhedral acicular aluminosilicate in clusters. (d-g), fine silicates particles (~ 1-2 µm) and, underneath, the glass surface is covered with a phyllosilicate showing a more fibrous morphology and a few fine particles (h).

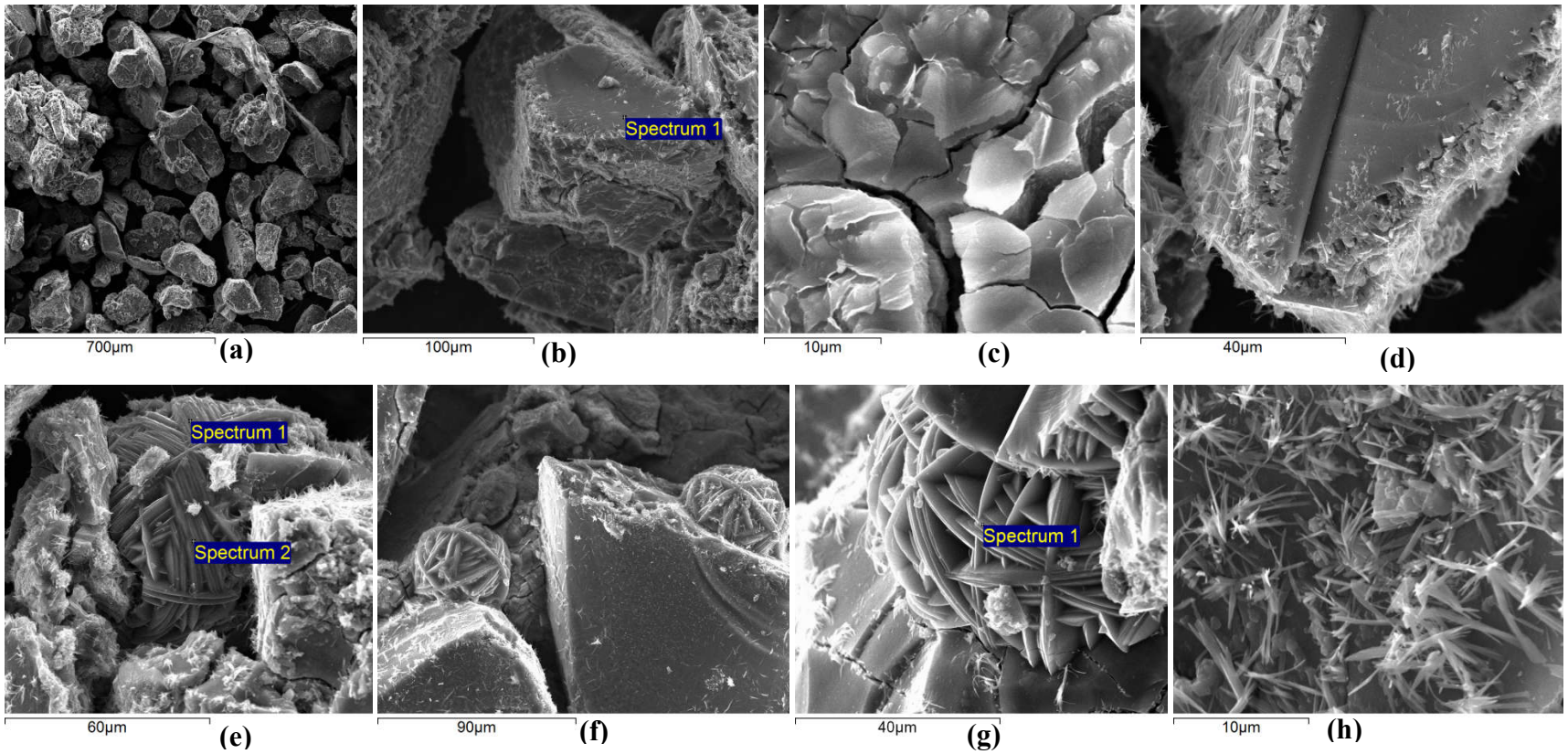

Figure 4.4. SEM micrographs of the surface of glass powder IDF18-A161CCC after 547 days of PCT-B at 90°C and 20,000 m^{-1} S/V; (a) the ~100 µm glass grains are inundated with finer particles, which could come from a spalled leached layer as evident in (b) or (c) and leached layer of about 15 to 20 µm seen in fractured glass grains (d). Two types of crystals are identified: a large (~60 µm) rosette shaped tectosilicate (e, f, g) and a fine (~ 1 µm) euhedral acicular aluminosilicate in clusters (h).

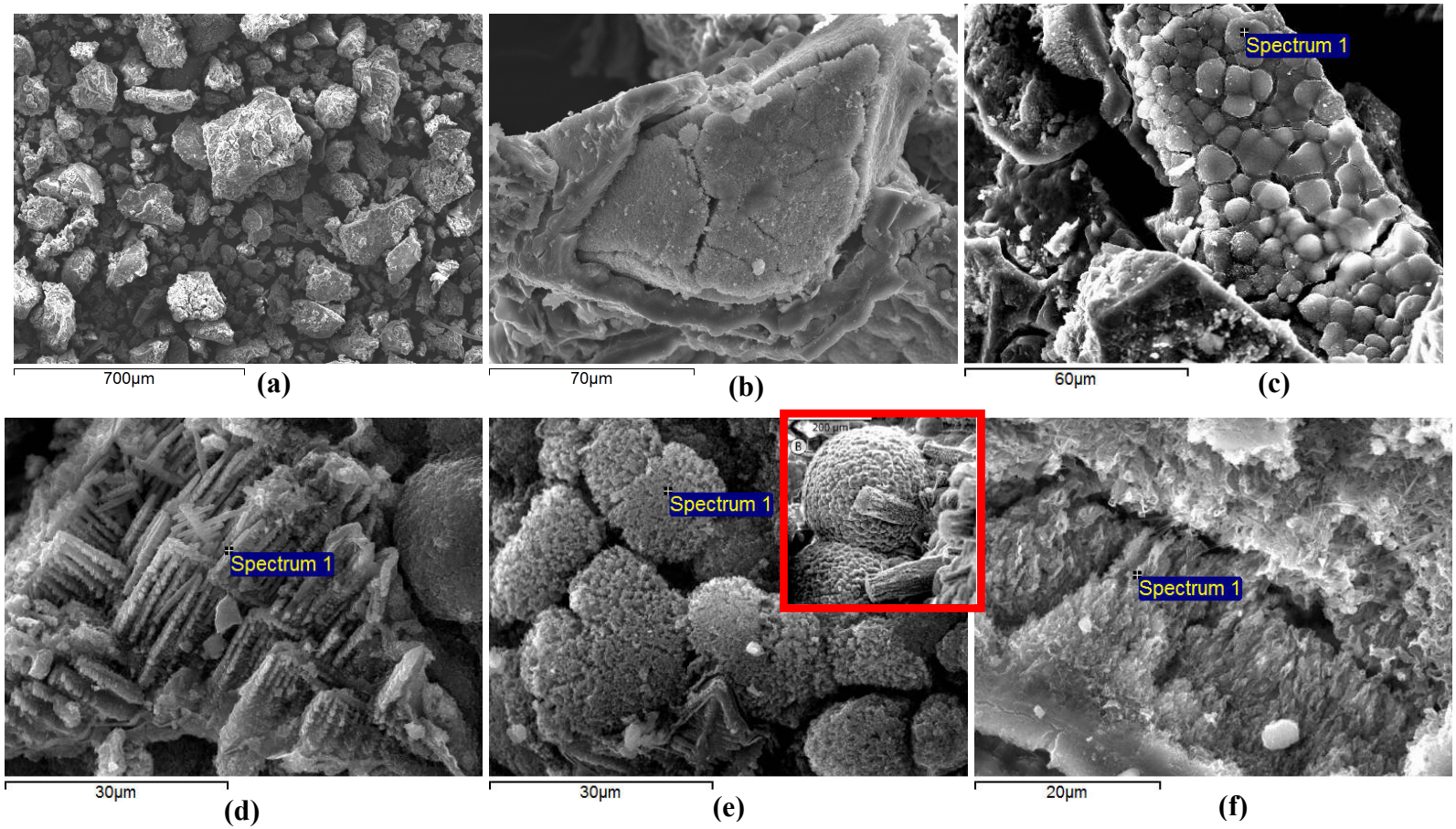

Figure 4.5. SEM micrographs of the surface of glass powder IDF19-C100CCC after 547 days of PCT-B at 90°C and 20,000 m^{-1} S/V; (a) the ~100 µm glass grains are inundated with finer particles and have clustered - a nearly 400 µm cluster is visible in (a). Some of the alteration gel may have fused the agglomerated grains, as evident in (b); the remaining glass and the leached layer of about 20 µm are both fractured (b, c). Two types of crystals are identified: a sub-euhedral, elongated and reticulated crystal (d) and a crystal in botryoidal clusters (c, e). A phase comparable to phillipsite seen in magmatic minerals alteration products [57] is shown in the red square inset. The alteration at the surface of the remaining glass shown in cross-section in (f) has evolved into a highly layered phyllosilicate.

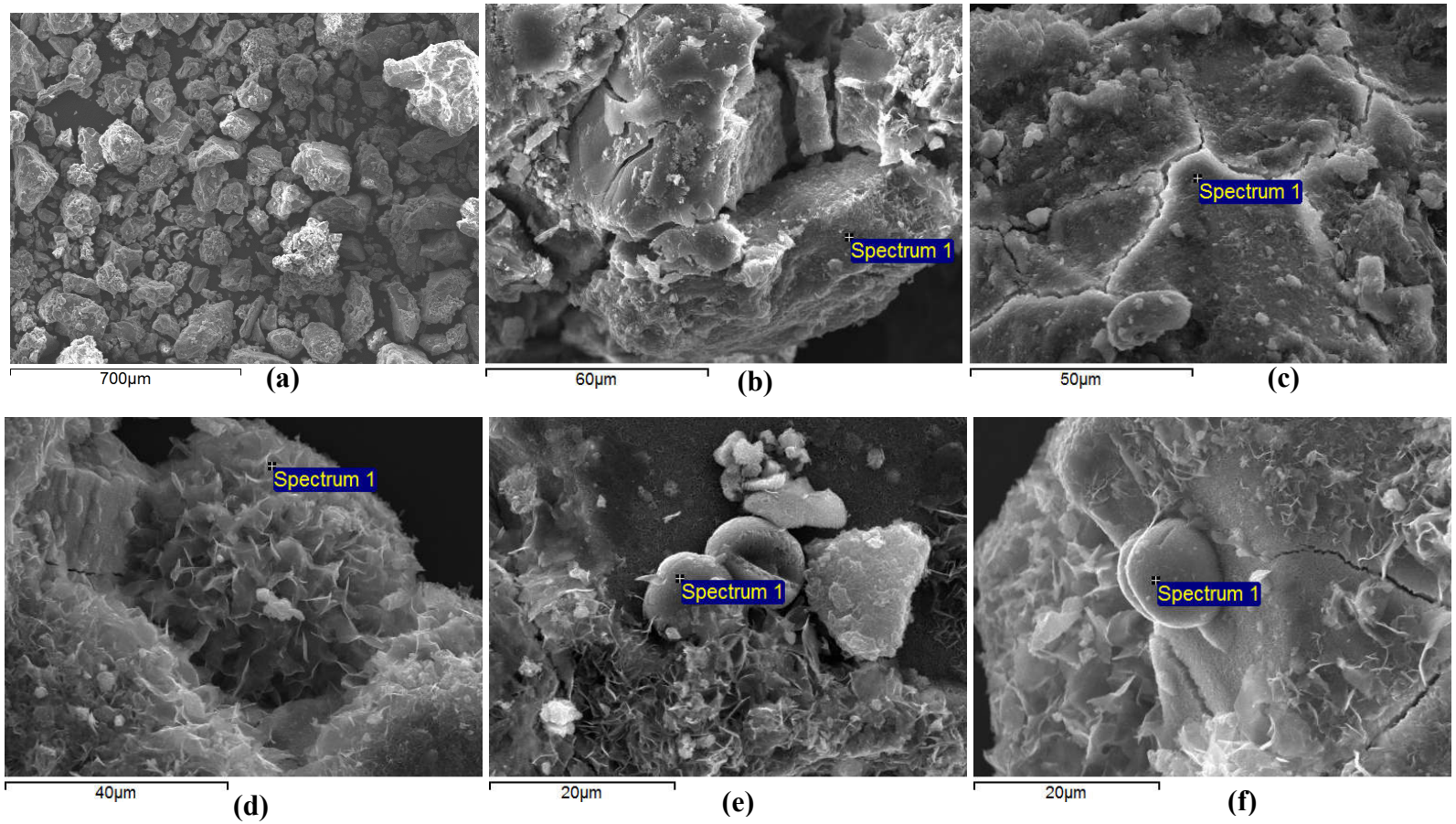

Figure 4.6. SEM micrographs of the surface of glass powder IDF20-F6CCC after 547 days of PCT-B at 90°C and 20,000 m^{-1} S/V; (a) the ~100 µm glass grains are covered with an alteration layer often fractured or spalled (as seen in b and c). Two types of crystals are identified: a flaky and fibrous crystal, which covers the glass surface and often clusters into radiating globular pattern (d), and rounded crystals of morphology and composition similar to hemimorphite (e, f). The surface is covered with the flaky layered phyllosilicate (f).

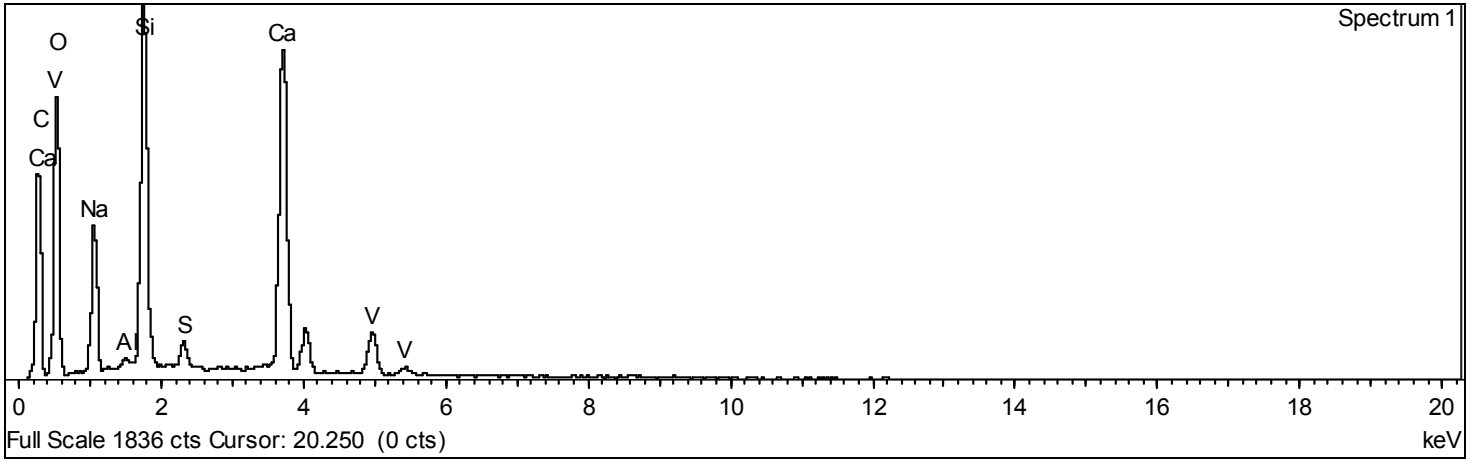

Figure 4.7. EDS of the fibrous crystal identified on the surface of IDF20-F6CCC (site (d) in Figure 4.6).

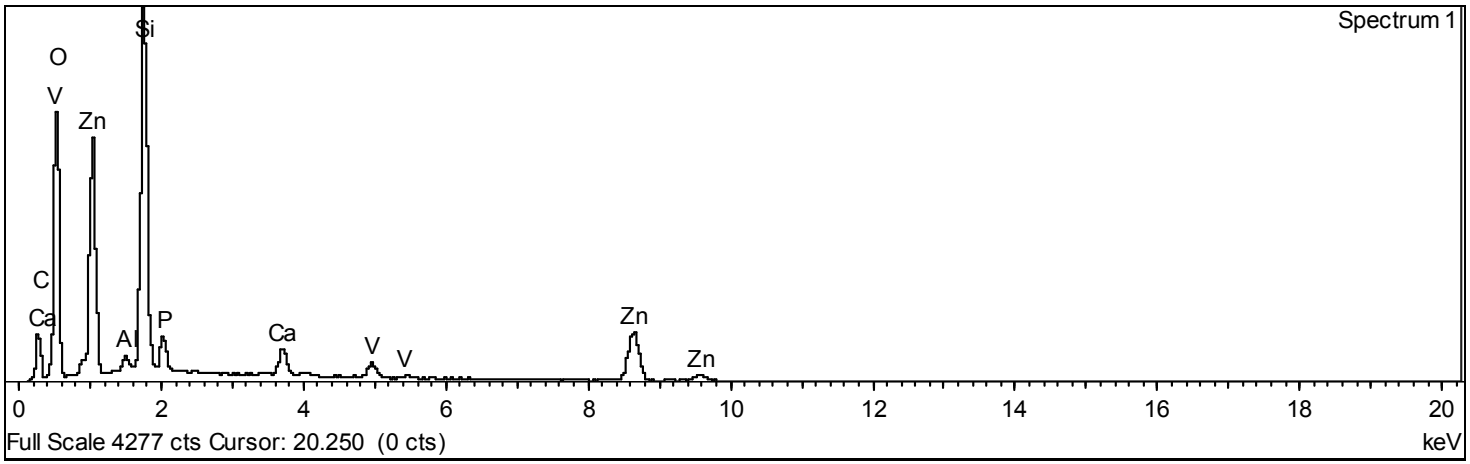

Figure 4.8. EDS of the zinc silicate identified on the surface of IDF20-F6CCC (site (f) in Figure 4.6).

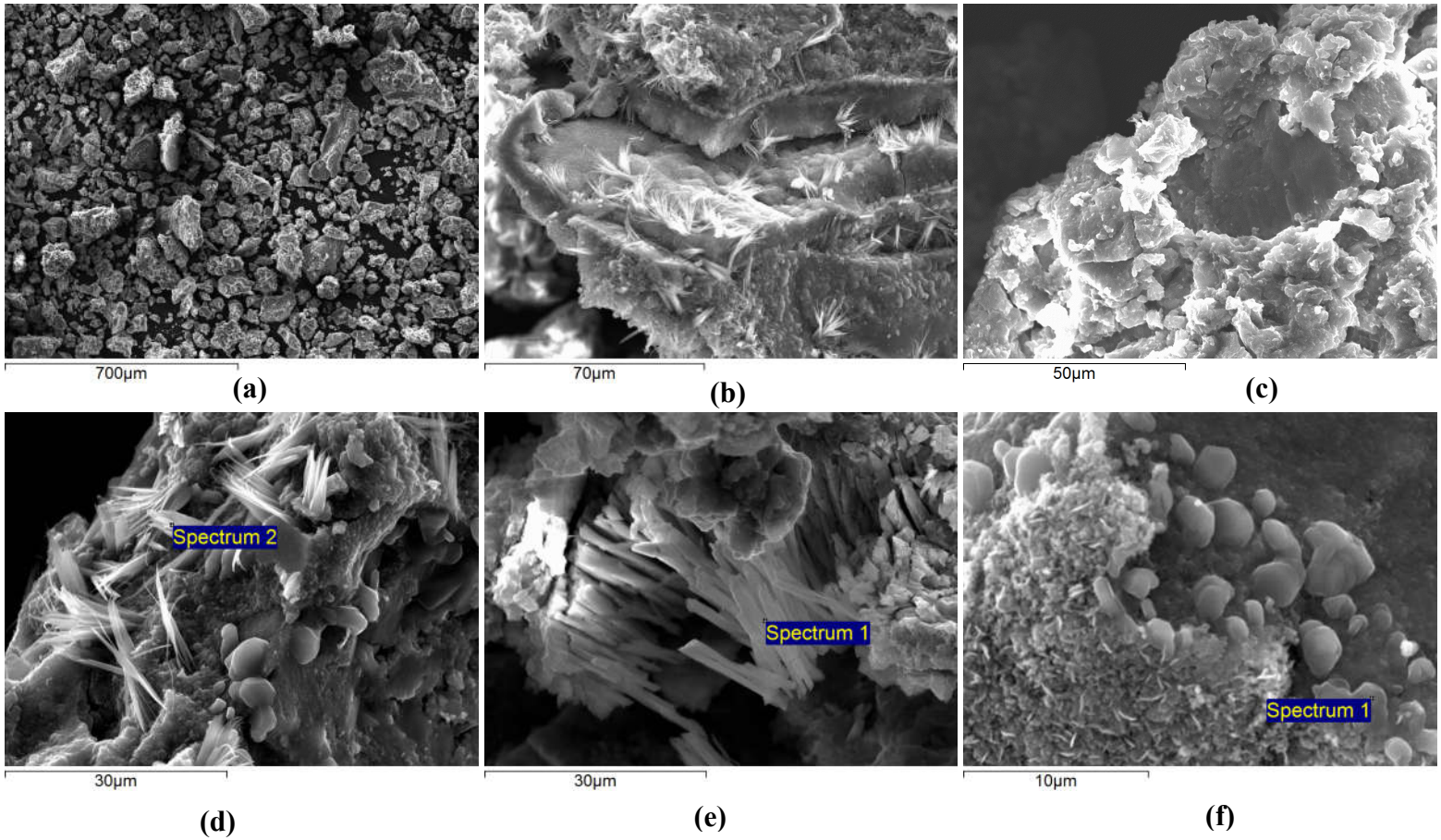

Figure 4.9. SEM micrographs of the surface of glass powder ANL-LRM2 after 547 days of PCT-B at 90°C and 20,000 m^{-1} S/V; (a) the ~100 µm glass grains are inundated with finer particles and often clustered (a). Spalled leached layer is evident in (b) and (c) and could be as thick as 15 to 20 µm (b). Three types of crystals are identified: a sub-euhedral, elongated and reticulated crystal (d), prismatic columns (e), and the ball-shaped phillipsite aggregate (f).

APPENDIX A

PCT-B Results for the Ten Phase 2 Glasses

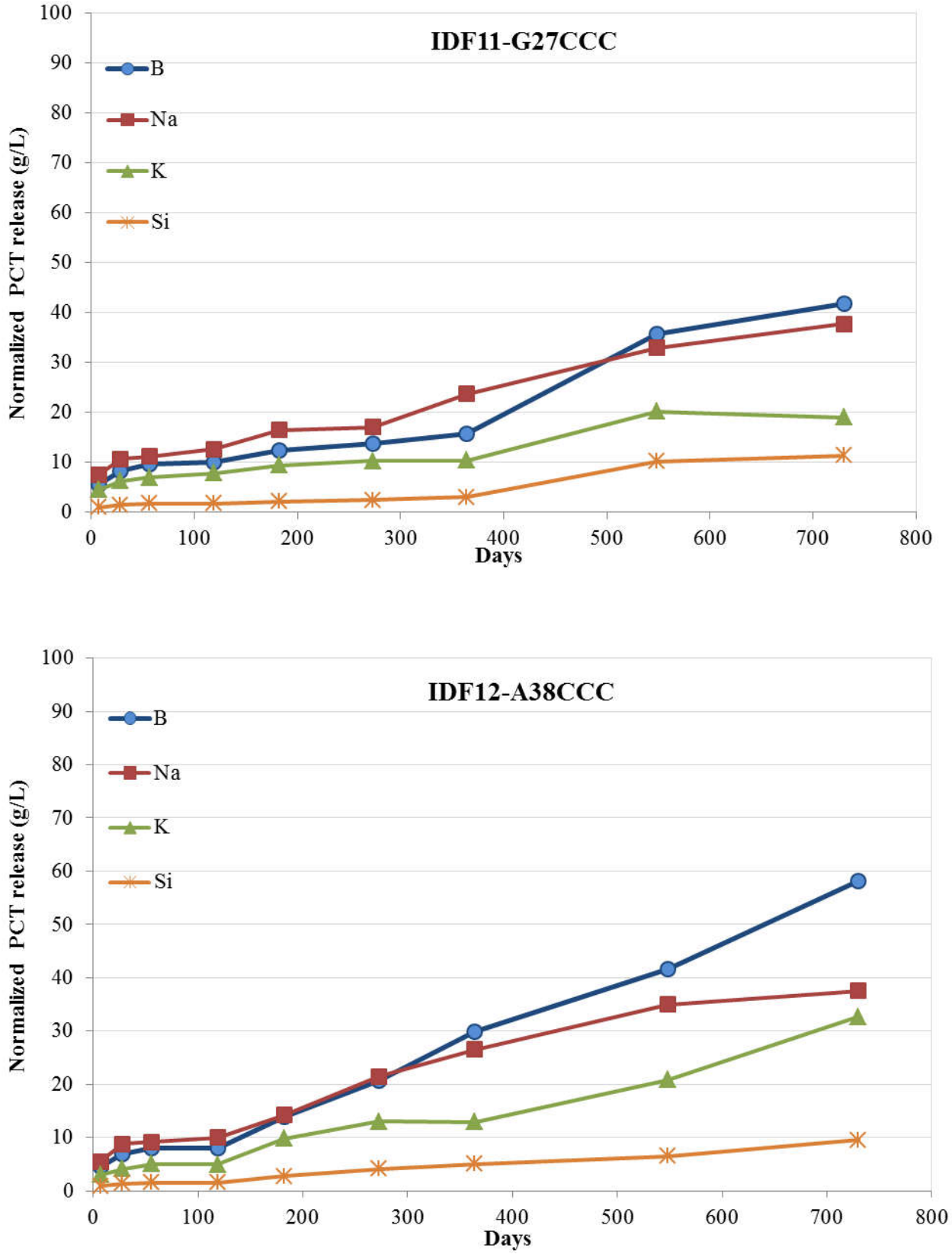

Figure A1. PCT-B Results for the Ten Phase 2 Glasses.

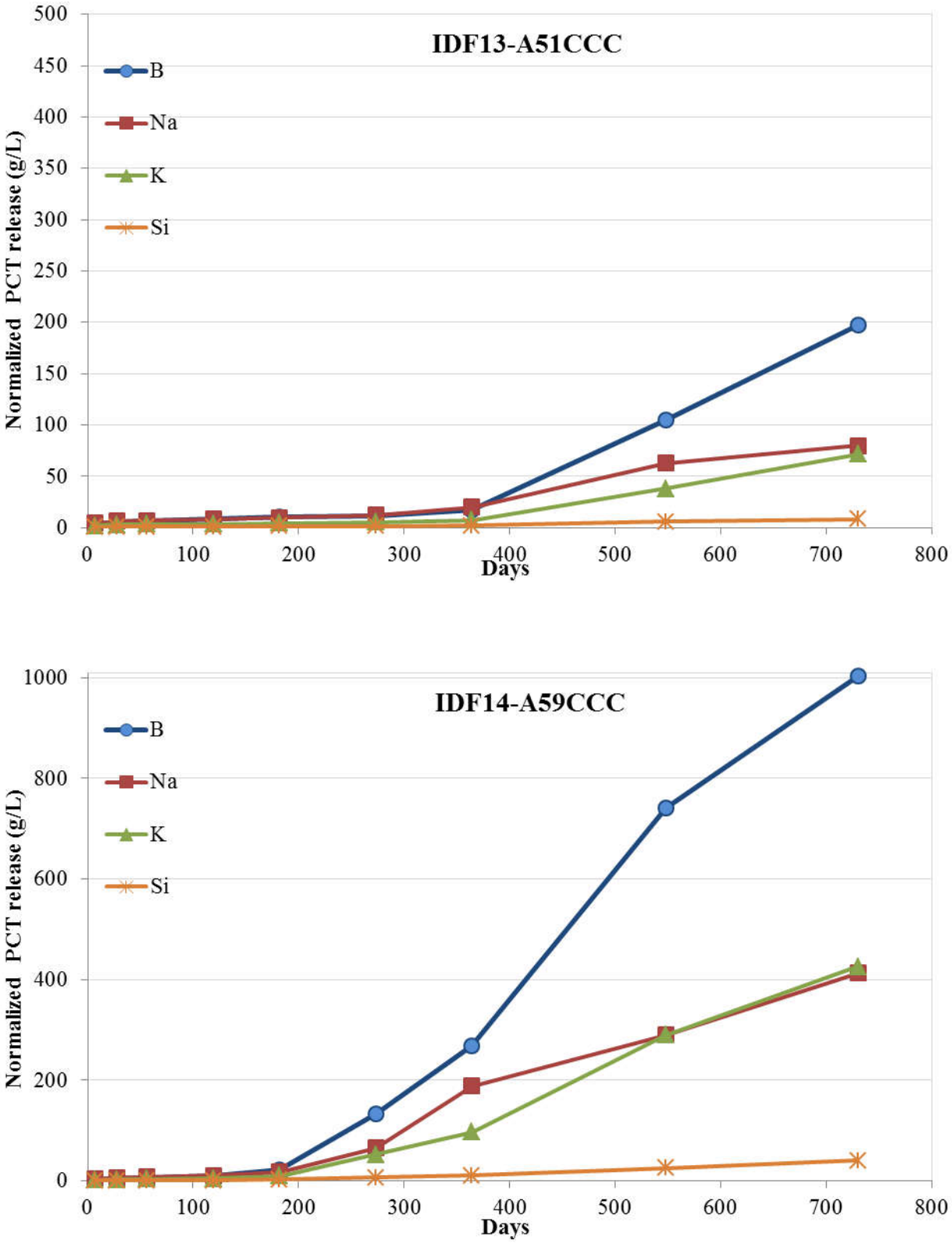

Figure A1. PCT-B Results for the Ten Phase 2 Glasses (continued).

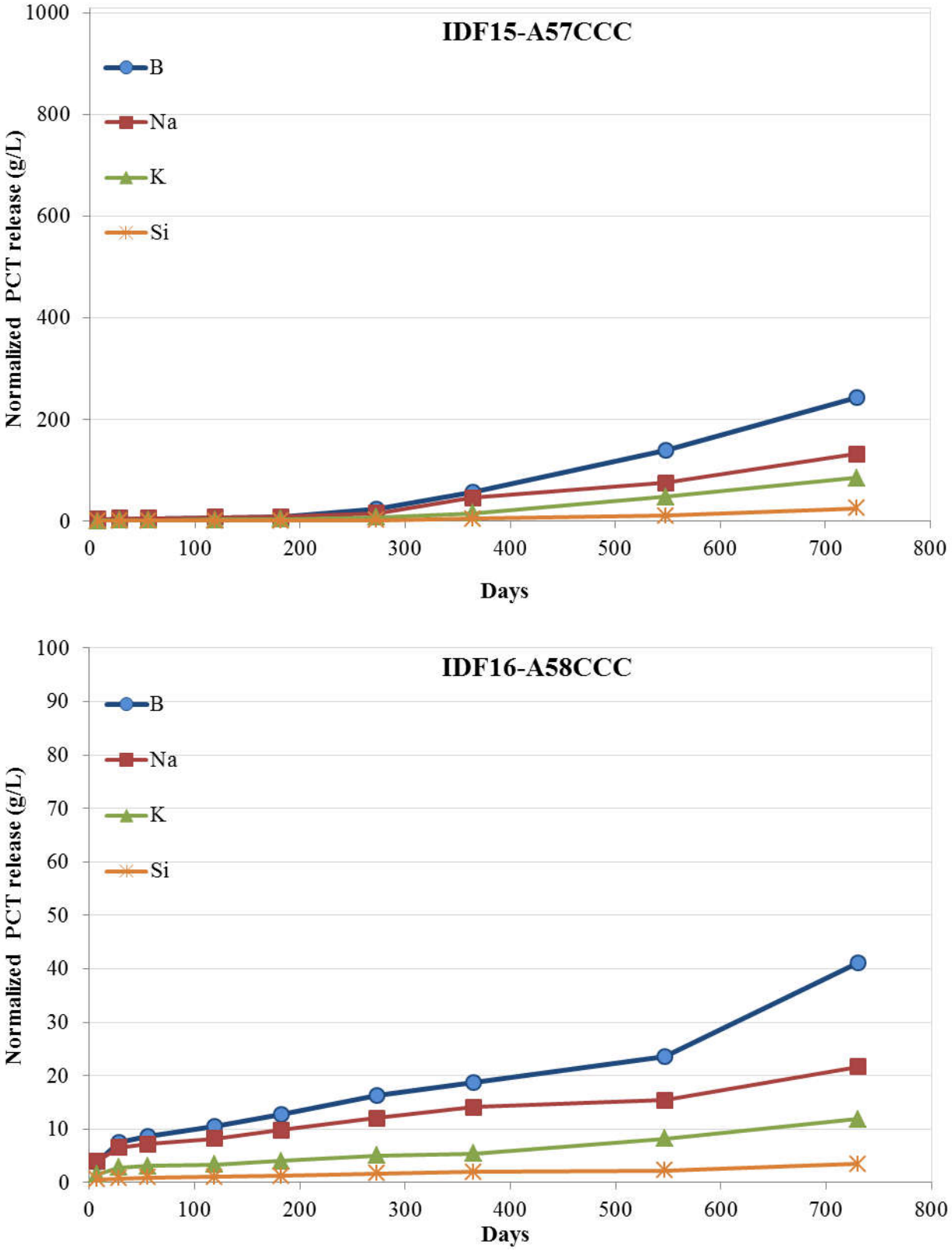

Figure A1. PCT-B Results for the Ten Phase 2 Glasses (continued).

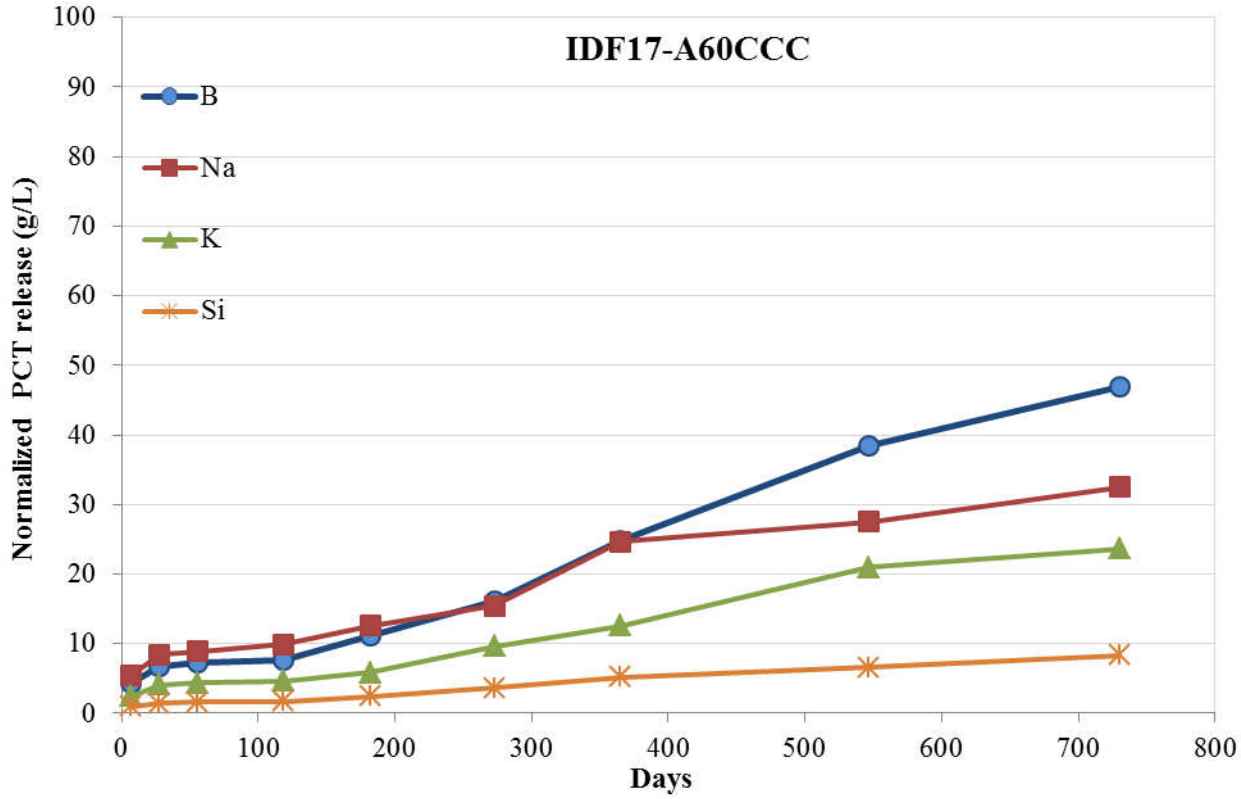

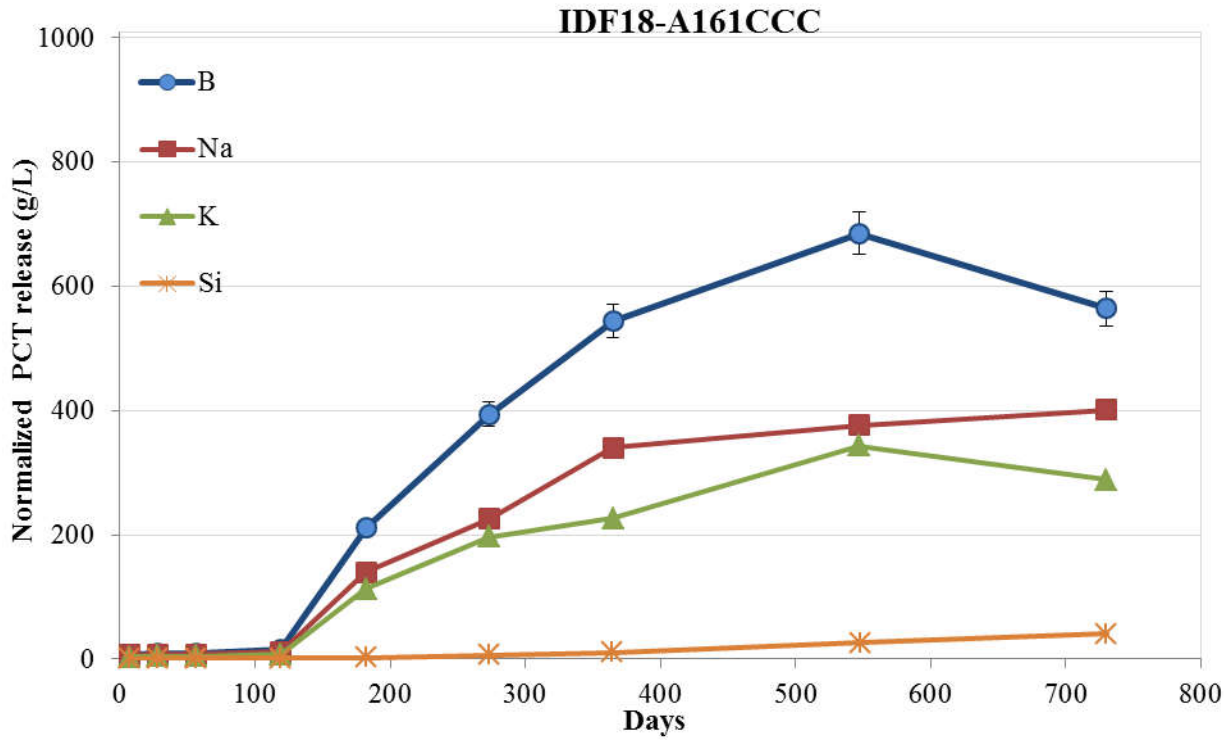

Figure A1. PCT-B Results for the Ten Phase 2 Glasses (continued).

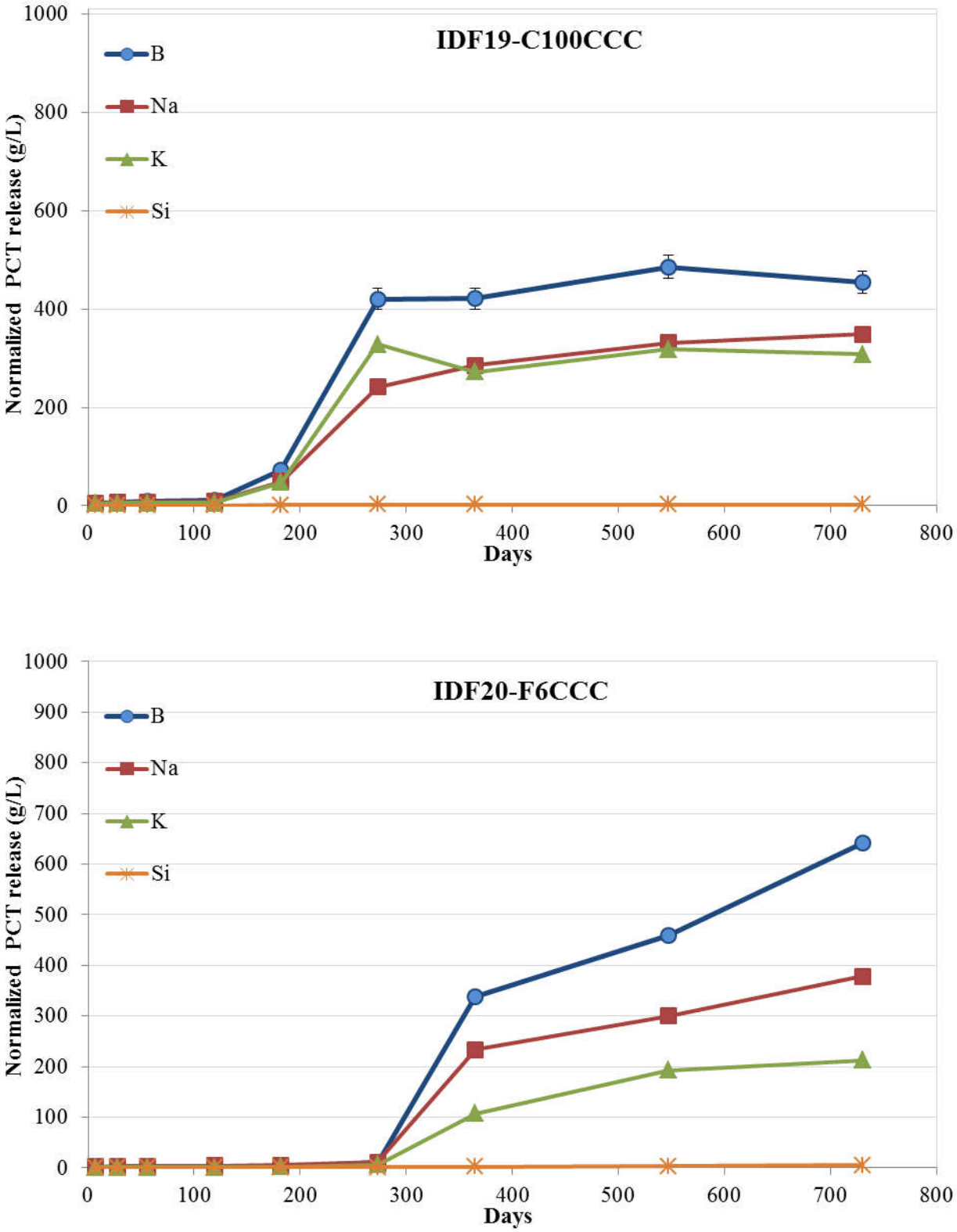

Figure A1. PCT-B Results for the Ten Phase 2 Glasses (continued).

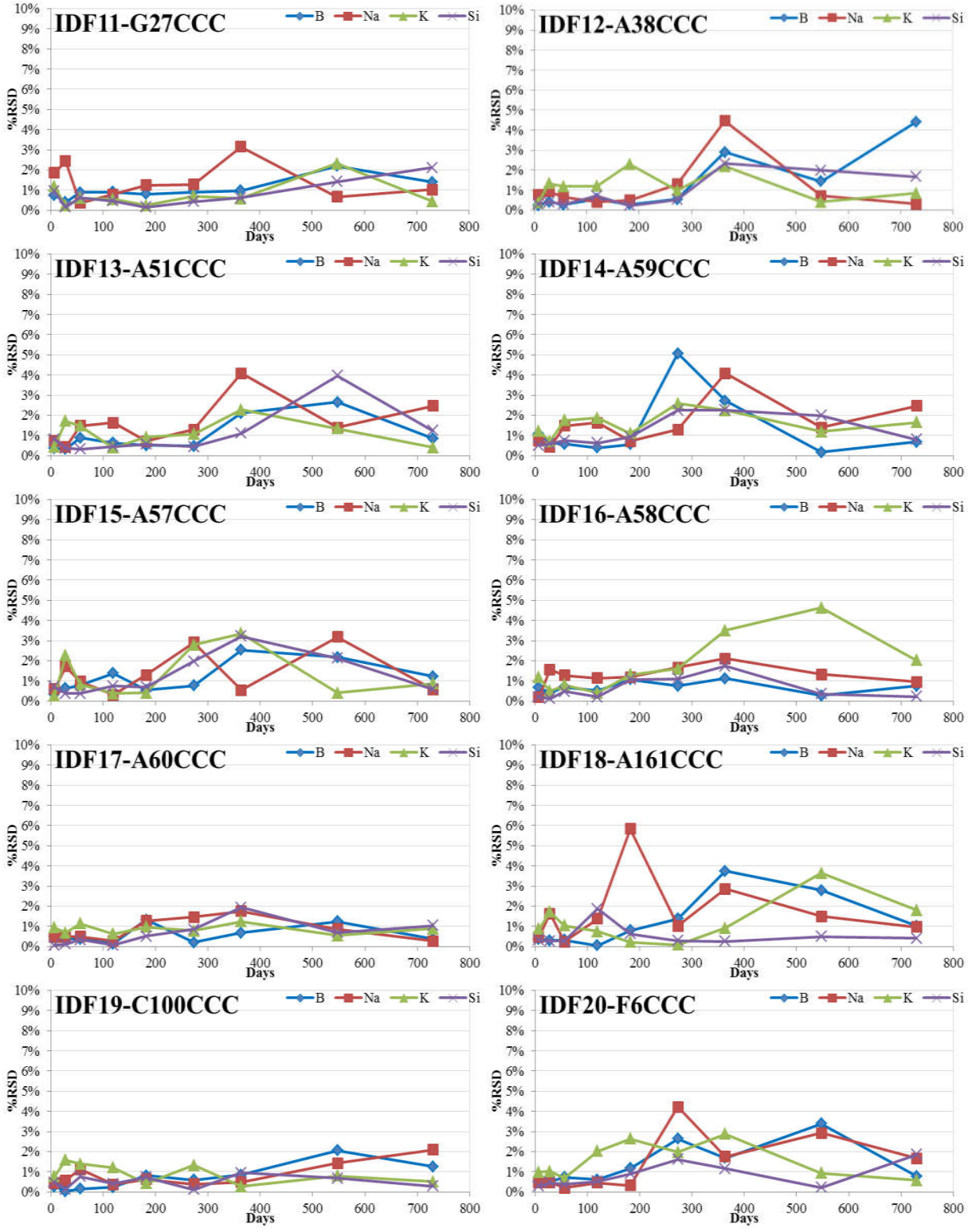

Figure A2. Percent RSDs for triplicate PCT release measurements.

APPENDIX B

Schematic diagram of a hectorite structure showing octahedral and tetrahedral sheets

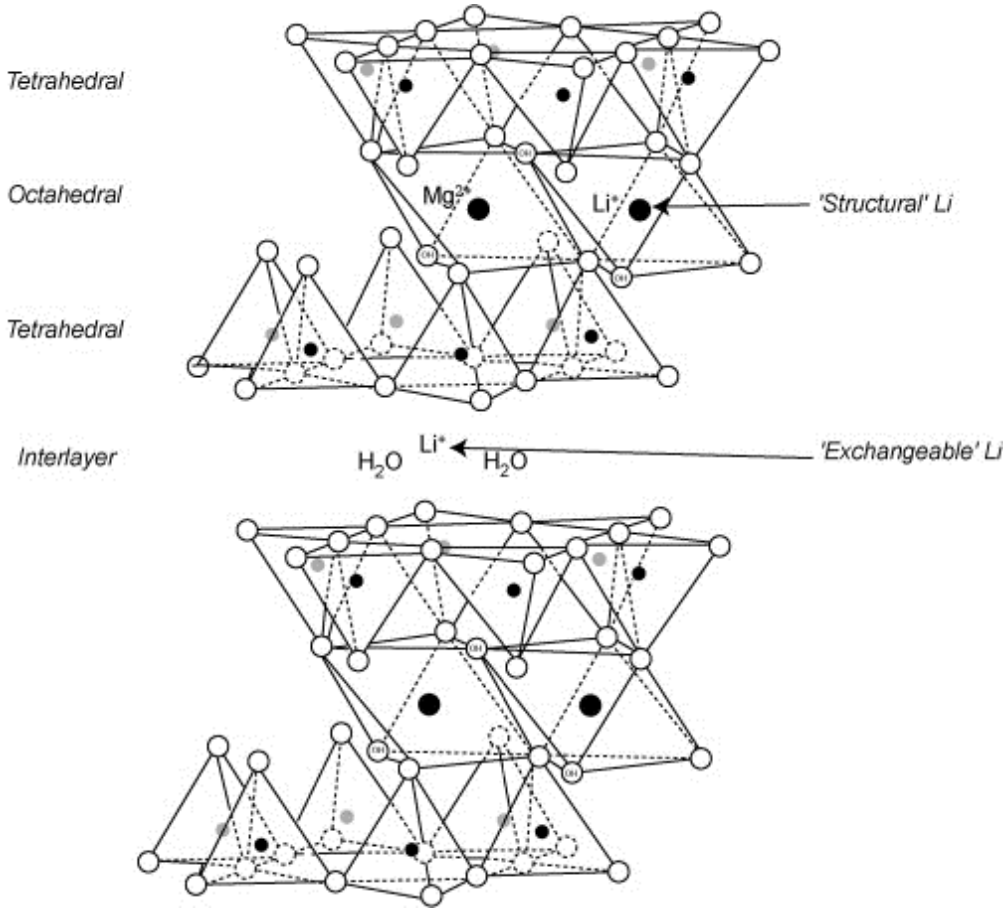

Figure 1 in "Quantifying Li isotope fractionation during smectite formation and implications for the Li cycle, N. Vigier, A. Decarreau, R. Millot, J. Carignan, S. Petit, and C. France-Lanord, Geochimica et Cosmochimica Acta, 72 (2008) 780–792.